VOL. 2. No. 9 SEPTEMBER 1937

Philips Technical Review

DEALING WITH TECHNICAL PROBLEMS
RELATING TO THE PRODUCTS, PROCESSES AND INVESTIGATIONS OF
N.V. PHILIPS' GLOEILAMPENFABRIEKEN

EDITED BY THE RESEARCH LABORATORY OF N.V. PHILIPS' GLOEILAMPENFABRIEKEN, EINDHOVEN, HOLLAND

FIVE-ELECTRODE TRANSMITTING VALVES (PENTODES)

by J. P. HEYBOER.

Summary. Following a general analysis of high-frequency amplification in transmitters, the characteristics of three-electrode, four-electrode and five-electrode valves are discussed, and the advantages of pentodes compared to four-electrode and three-electrode valves enumerated.

Introduction

High-vacuum amplifying valves are used in radio transmitters for various purposes, which may be classified under the following heads:

a) As low-frequency amplifiers,
b) As high-frequency amplifiers, and
c) As oscillators.

The first of these groups is used for the amplification of speech and music which are superposed as a modulation on the high-frequency carrier wave; for this reason these valves are sometimes also described as "modulating amplifiers".

The valves in groups b) and c) form components of the high-frequency part of the transmitter, while the oscillator is used for generating the required high-frequency oscillation which is then amplified in the succeeding high-frequency amplifiers.

The present article is limited to a discussion of high-frequency amplifiers.

A, B and C Amplification

If, for a particular amplifying valve, the anode current is measured as a function of the control-grid voltage, the potentials of the other electrodes being kept constant, a characteristic is obtained of the type shown diagrammatically in *fig. 1.*

When the valve is used as an amplifier, a certain negative bias is applied to the grid, which is superposed on the alternating voltage to be amplified.

Three types of amplification are distinguished according to the magnitude of the negative bias, viz.:

Class A amplification,
Class B amplification, and
Class C amplification.

Class A amplification is obtained when the negative bias is such that anode current still flows when the alternating grid voltage is zero and does not disappear even with the maximum negative

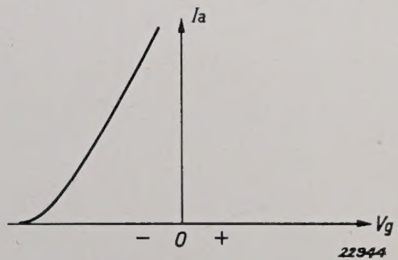

Fig. 1. Static characteristic of an amplifying valve with the anode current I_a plotted as a function of the control-grid voltage V_g.

amplitude of the alternating grid voltage occurring. This signifies that anode current flows during the full cycle of the alternating voltage applied to the grid.

With class B amplification the grid bias is so adjusted that the flow of anode current in the absence of a signal is nearly zero. If the bias voltage is superposed on the alternating voltage to be amplified, anode current will flow during half the cycle only.

In class C amplification the grid bias is more negative still than in the previous case; in the absence of a signal the anode current is zero, and when an alternating voltage is impressed on the grid, current will flow during a part of a half-cycle only.

If the alternating voltage at the grid varies sinusoidally with the time, the anode current can be readily determined, on the basis of fig. 1, as a func-

tion of the time for each of the three classes of amplification. The results obtained in this way are shown in *fig. 2*.

The curves in fig. 2 show that in class A ampli-

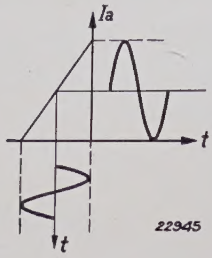

Fig. 2. Anode current plotted as a function of the time, on excitation of the control grid with a sinusoidal voltage, with *a)* Class A amplification

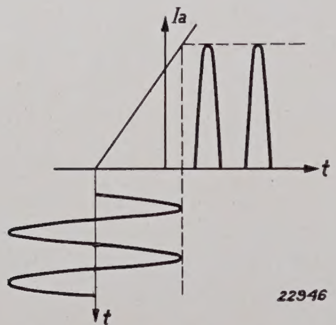

b) Class B amplification

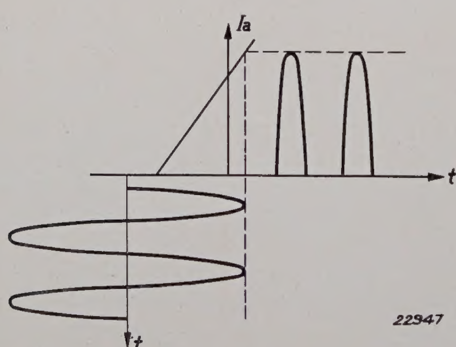

c) Class C amplification

fication the anode current has almost the same curve as the grid voltage; this is not the case with class B and class C amplification because in the negative half-cycle no current flows. Class A amplification has, therefore, been favoured for low-frequency amplifiers in which undistorted reproduction of speech and music is a first consideration.

Class A amplifiers have, however, the disadvantage that a feed current continues to flow through the anode even in the absence of a signal voltage at the grid, the power carried by this current being dissipated in the form of heat. Since during operation of the valve the anode current fluctuates about this residual value, the efficiency is somewhat reduced. The maximum efficiency found with class A amplifiers is actually only of the order of 50 per cent, in other words 50 per cent of the D.C. power absorbed is transformed to useful work, while the remainder is dissipated at the anode as heat.

While this dissipation in the form of heat has frequently to be taken into account with receiving valves, its consideration is imperative in the case of transmitting valves owing to the heavy powers with which these valves have to deal, and the large monetary loss entailed in the loss of power. It is extremely important, therefore, to increase the efficiency of transmitting valves as far as practicable in order to obtain the maximum power output with a specified permissible anode dissipation. This result may be obtained in class B and class C amplification, as will be described in further detail below.

Power Output and Efficiency with Class B and Class C Amplification

The standard circuit of a high-frequency amplifier is shown in *fig. 3*. The grid is given such a high

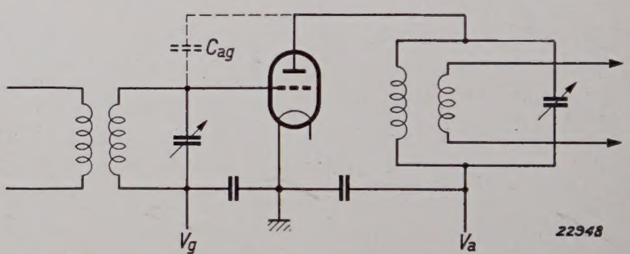

Fig. 3. Circuit using a three-electrode valve as a high-frequency amplifier. Owing to the capacity C_{ag} between the grid and anode, part of the alternating anode current is passed through the input circuit; when this circuit has an inductive reactance this may give rise to self-excitation.

negative bias that the anode current is zero (class C) or nearly zero (class B) in the absence of a signal. This negative grid bias is superposed on the high-frequency alternating voltage, which is furnished by the preceding stage in the transmitter and which is termed the exitation voltage.

A circuit is inserted in the anode lead of the valve having a resistance as load (e.g. the radiation resistance of an aerial) and which is tuned to the frequency of the excitation voltage.

Plotted as a function of the time, the anode current gives a curve of the form shown diagrammatically in figs. 2*b* (class B) and 2*c* (class C).

This current curve can be resolved into a D.C. component and various high-frequency components, as shown in *fig. 4* for a specific curve obtained with Class C amplification.

One of the high-frequency components has the

same frequency as the excitation voltage (the fundamental frequency), while the other components have frequencies which are multiples of the fundamental frequency.

The anode circuit is tuned to the fundamental frequency; this implies that only those current

$$P_0 = {}^1/_2\, I_{a1}\, V_{a\sim}, \quad \cdot \cdot \cdot \cdot \quad (2)$$

while the D.C. power absorbed is:

$$P_i = V_a\, I_{a0}, \quad \cdot \cdot \cdot \cdot \cdot \cdot \quad (3)$$

where V_a is the direct anode voltage and I_{a0} the direct anode current.

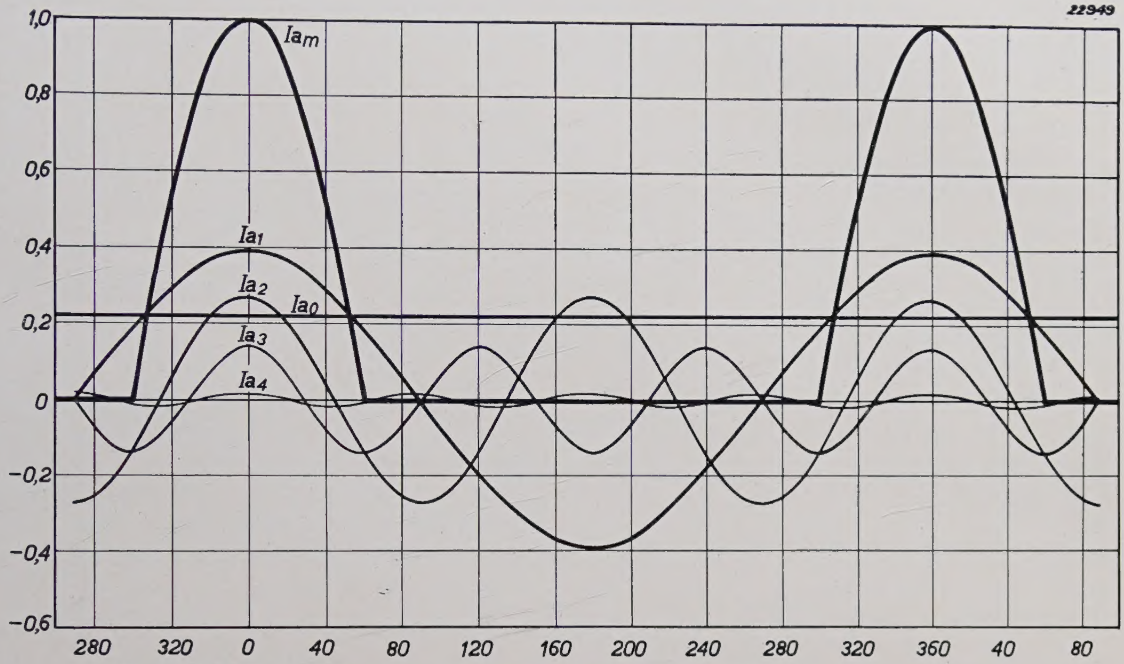

Fig. 4. Resolution of the anode-current curve of a class C amplifier into D.C. components and harmonics, when the current-carrying period is one third of the full cycle and the valve characteristic is linear.

components having the fundamental frequency (the first harmonic) encounter an impedance, which is moreover ohmic in character and which we shall term R_a, while no impedance is provided for the other harmonics. Only the first harmonic of the anode current, whose amplitude will be denoted by I_{a1}, will therefore produce a voltage drop across the resistance, this voltage drop being sinusoidal with an amplitude which will be denoted by $V_{a\sim}$. It is clear that I_{a1} and $V_{a\sim}$ are connected by the following expression:

$$V_{a\sim} = I_{a1}\, R_a \quad \cdot \cdot \cdot \cdot \cdot \cdot \quad (1)$$

From fig. 4 it is evident that the maximum of the first harmonic occurs simultaneously with the maximum I_{a_m} on the total anode-current curve. Since the maximum anode current naturally coincides with the maximum grid voltage $V_{g\sim}$, I_{a1} and $V_{g\sim}$ are cophasal. It follows from the fact that $V_{a\sim}$ is a voltage drop in R_a that $V_{a\sim}$ is in phase opposition to $V_{g\sim}$. The variations of the currents and voltages with time are shown in *fig. 5*.

The power passing from the valve to the anode resistance R_a is:

The efficiency is therefore:

$$\eta = \frac{P_0}{P_i} = {}^1/_2\, \frac{I_{a1}}{I_{a0}} \cdot \frac{V_{a\sim}}{V_a}; \quad \cdot \cdot \cdot \quad (4)$$

and is thus determined by the ratios I_{a1}/I_{a0} and $V_{a\sim}/V_a$, the latter ratio being termed the voltage

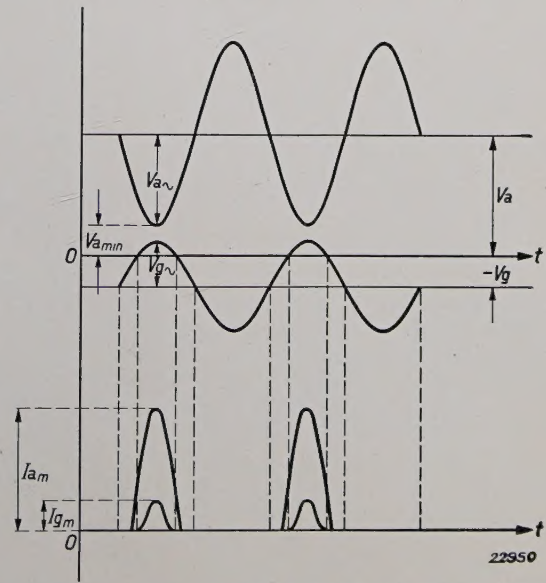

Fig. 5. Voltages and currents plotted as a function of the time for a class C amplifier.

amplification factor. A higher efficiency is therefore obtained when the ratios I_{a1}/I_{a0} and $V_{a\sim}/V_a$ are made as large as possible.

The ratio I_{a1}/I_{a0} is determined by the shape of the anode current curve and for a given form of curve may be found by expanding in a Fourier series.

If the curve is composed of semi-sinusoidal components (half-waves), as is nearly the case with Class B amplification, the ratio $I_{a1}/I_{a0} = {}^1/_2\,\pi = 1.57$; with class C amplification this ratio has a greater value and is usually between 1.7 and 1.8.

The voltage amplification factor $V_{a\sim}/V_a$ cannot in practice exceed unity and is usually about 0.9. (With four-electrode valves the conditions are somewhat different, as will be shown below). Why the amplification factor has this value may be explained as follows:

When the grid bias passes through its maximum value, the anode current is also a maximum and the anode voltage is a minimum. The residual anode voltage is then:

$$V_{a_{\min}} = V_a - V_{a\sim} \quad \cdots \cdot \quad (5)$$

(see fig. 5).

When the ratio $V_{a\sim}/V_a$ approaches unity, $V_{a_{\min}}$ becomes steadily smaller, finally becoming zero, and even negative when $V_{a\sim}/V_a$ is slightly greater than 1. If, however, $V_{a_{\min}}$ is zero or negative, the anode current must be zero, since the electrons are now no longer accelerated in the direction of the anode, but on the other hand are thrown back towards the grid after having passed through it. Instead of a maximum, the anode current then passes through a minimum value, so that the current curve is of the form shown diagrammatically in *fig. 6*, i.e. at the point where a maximum was

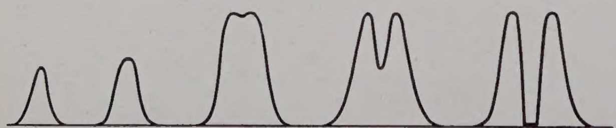

22351

Fig. 6. Variation of the anode current of a three-electrode valve with sinusoidal excitation voltage (increasing from left to right). If the excitation voltage is so high that the anode voltage drops below the grid voltage at the peak value of the anode current, the greater part of the emission current passes to the grid at the expense of the anode current. This produces a trough in the current curve of such character that the first harmonic of the anode current no longer increases above a certain excitation voltage.

previously obtained the curve is now troughed, the trough being the deeper the smaller $V_{a_{\min}}$, in other words the greater $V_{a\sim}$ becomes.

The presence of this trough imposes a certain limit on all components of the anode current, as for instance on the first harmonic I_{a1}, since its maximum happens to be located just at the trough. As equation (1) is valid throughout, $V_{a\sim}$ also has a limit, which according to experience is about 0.9 of the direct anode voltage. We thus find that the alternating anode voltage is limited by the direct anode voltage.

Since the voltage and current amplification factors are now approximately known, the same also applies to the efficiency; for class B amplifiers the efficiency is about 70 per cent and for class C amplifiers 75 to 80 per cent.

It is seen that the efficiency is considerably higher than with Class A amplifiers.

Three-Electrode Valves as High-Frequency Amplifiers

If a three-electrode valve is used as a high-frequency amplifier in the manner described, a high power output as well as a satisfactory efficiency is obtained.

There are, however, two important disadvantages in this use of the three-electrode valve, viz.:

1) The control grid current is comparatively high, and
2) The valve is liable to become self-exciting.

Regarding the control grid current, it should be noted that the magnitude of this current is closely associated with the voltage amplification factor. We have seen (fig. 5) that the anode voltage is a minimum at the same time as the grid voltage is a maximum, and also that the alternating anode voltage must be made as high as possible in order to obtain a satisfactory efficiency. But the increase in the voltage amplification factor will be limited merely to making the minimum anode voltage equal to the maximum grid voltage. If, for instance, the grid voltage were higher than the anode voltage, then during the time in which the grid is at this potential a large part of the emission current would flow from the cathode to the grid at the expense of the anode current. This would naturally reduce the power output, since the trough in the anode current curve is then produced as already described, while the grid current curve would exhibit a high peak.

The minimum anode voltage must, therefore, never be smaller than the maximum grid voltage, but at most equal to it; with larger valves, especially those of the water-cooled type, the minimum anode voltage is in fact a multiple of the maximum grid potential.

Nevertheless, even when this condition is met, the grid current will still be fairly high, since owing to

the periodically low anode voltage the accelerating action of the anode is small and hence the probability of electrons reaching the grid is comparatively high.

The grid current power, the socalled excitation power, is hence relatively high with a three-electrode valve and must be furnished by the preceding stage. It will be seen below that screen grid valves have more satisfactory characteristics in this direction.

The liability to become self-exciting is due to the capacity between the grid and anode, shown as C_{ag} in fig. 3, because the alternating anode voltage induces a current in the series circuit made up of C_{ag} and the grid circuit, whereby an alternating voltage is applied to the latter. If the impedance in the grid circuit is inductive, this feed-back voltage will be in phase opposition to the alternating anode voltage and hence just cophasal with the initial excitation voltage. In certain circumstances, the feed-back voltage at a given alternating anode voltage can thus become equal to the excitation voltage required to produce this alternating anode voltage; self-excitation then results.

This disadvantage of high-frequency three-electrode amplifiers can be eliminated in one of two ways:

1) By neutrodyning, i.e. applying a voltage to the grid which is equal to the feed-back voltage but in phase opposition to it.
2) Inserting an auxiliary grid between the anode and control grid, which is earthed on the high-frequency side, so that a screening action is produced between the anode and the control grid, and C_{ag} is thereby made very small.

Four-Electrode Valves

The latter method is used in four-electrode and five-electrode valves which are fitted with a screen grid g_2 between the control grid g_1 and the anode a. Experience has shown that neutrodyning can be dispensed with in these amplifying valves, as C_{ag_1} is very small. The values of C_{ag_1} are given below for typical four-electrode valves, as well as the corresponding values for two-three-electrode valves for purposes of comparison.

Four-electrode valves	QC 05/15	$C_{ag_1} = 0.004$ μμF
	QB 2/75	$C_{ag_1} = 0.02$ μμF
	QB 3/500	$C_{ag_1} = 0.01$ μμF
Three-electrode valves	TC 04/10-I	$C_{ag} = 6.8$ μμF
	TC 1/75	$C_{ag} = 10.4$ μμF

The introduction of the screen grid alters the shape of the anode-current/anode-voltage characteristics, so that these curves differ from those for three-electrode valves. This is shown by the characteristics for a TC 04/10 three-electrode valve and a QC 05/15 four-electrode valve in *figs. 7* and *8*,

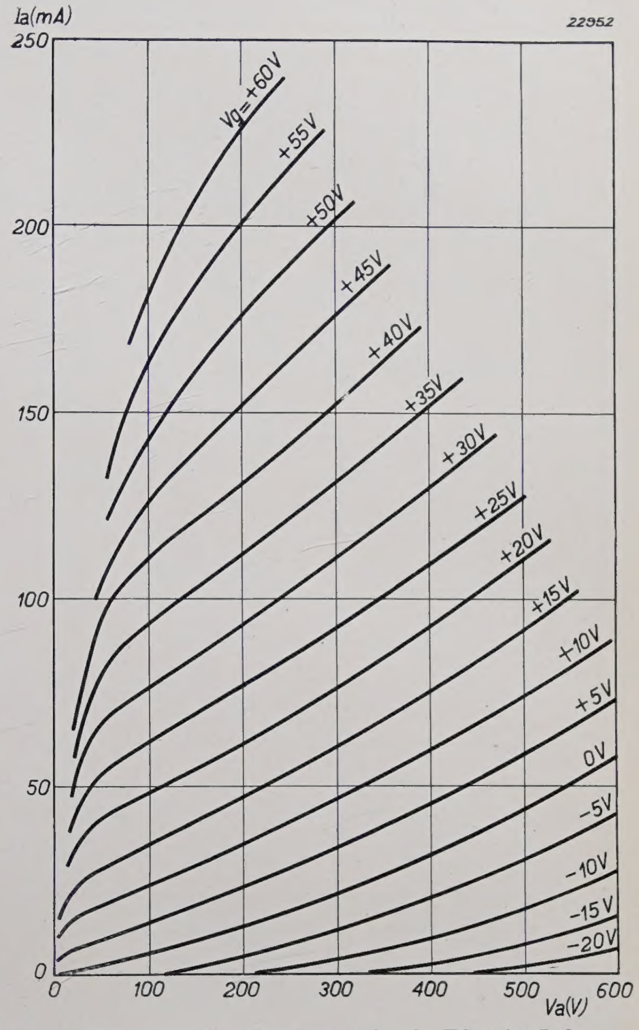

Fig. 7. Static I_a - V_a characteristic for the TC 04/10-I three-electrode valve. The anode current increases sharply with the anode voltage.

where by far the greater parts of the characteristics for the four-electrode valve are nearly parallel to the V_a axis, in other words the anode current is practically independent of the anode voltage. That this must in fact be the case is self-evident, for the screening effect produced by the screen grid practically eliminates the influence of the anode voltage on the anode current.

It may be seen from fig. 8 that the I_a-V_a characteristics of a four-electrode valve rapidly drop to zero, when the anode voltage is roughly equal to the screen grid voltage. As a result, the alternating anode voltage during operation can at most become equal to the difference between the direct

voltages at the anode and screen grid, since the anode-current curve becomes troughed in the way already described when the alternating voltage increases. The voltage amplification factor cannot here reach unity but is approximately equal to

$$\frac{V_{a\sim}}{V_a} = \frac{V_a - V_{g_2}}{V_a} = 1 - \frac{V_{g_2}}{V_a} \quad . \; . \; . \; (6)$$

If V_{g_2} is large in comparison with V_a, as occurs for instance in the QC 05/15 valve, where V_a = 500 volts and V_{g_2} = 125 volts, the amplification factor will be much less than 1 (e.g. in the QC 05/15 valve about 0.75). The power output and the efficiency are therefore both reduced.

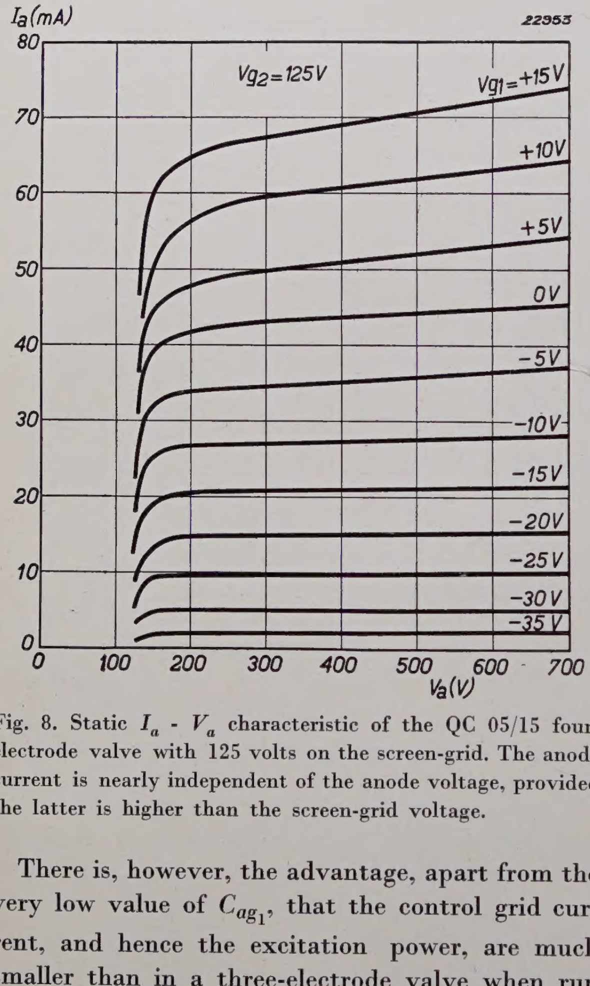

Fig. 8. Static I_a - V_a characteristic of the QC 05/15 four-electrode valve with 125 volts on the screen-grid. The anode current is nearly independent of the anode voltage, provided the latter is higher than the screen-grid voltage.

There is, however, the advantage, apart from the very low value of C_{ag_1}, that the control grid current, and hence the excitation power, are much smaller than in a three-electrode valve when run under otherwise equivalent conditions, so that the control stage can be given a much smaller rating and is therefore cheaper to make.

The fact that the control grid current is low is due to the presence of the screen grid to which a constant high potential is applied, while a similarly high voltage is not applied to the control grid during the working of the valve. The accelerating force applied to the electrons after passing through the control grid is, in consequence, greater than in a three-electrode valve; so that relatively less electrons pass to this grid and the grid current is lower.

Secondary Emission

The bend in the I_a-V_a characteristics of a four-electrode valve at the point $V_a = V_{g_2}$ is due to secondary emission at the anode and screen grid.

Of the electrons penetrating the control grid a part will strike the screen grid and others will pass to the anode. By the impact of the (primary) electrons secondary electrons are emitted from the screen grid, which travel towards the anode as long as its potential is higher than of this grid. If, on the other hand, the anode voltage is made equal to the screen grid voltage or slightly higher than the latter, practically no accelerating force towards the anode will be applied to the secondary electrons emitted from the screen grid and these will therefore not reach the anode. Should the anode voltage be lower than the screen grid voltage, the secondary electrons liberated from the anode will on the contrary pass to the screen grid, with the result that the anode current may even become negative.

Five-Electrode Valves (Pentodes)

To suppress secondary emission, a third or suppressor grid connected to the cathode has been interposed between the screen grid and the anode in pentodes. The secondary electrons from the screen grid are now unable to reach the anode owing to their low velocity and the repulsion applied by the suppressor grid. There is just a little opportunity for secondary electrons from the anode to travel to the screen grid, when V_a and V_{g_2} become smaller. This also eliminates the marked reduction of I_a in the neighbourhood of $V_a = V_{g_2}$. In fact the I_a-V_a characteristics of pentodes are nearly parallel to the V_a axis up to almost V_a = 0, as is shown in *fig. 9* for the PE 05/15 pentode.

Only when the anode voltage approaches zero does a bend appear in the characteristics, because then the primary electrons which have passed through the screen grid are no longer accelerated and the anode current hence drops to zero.

Thus when using a pentode as a high-frequency amplifier, the maximum value reached by the alternating anode voltage is roughly equal to the direct anode voltage, so that the voltage amplification factor again approaches unity and is hence higher than with a four-electrode valve other conditions being equal. The power output and efficiency are therefore also higher.

The advantages of the pentode may be summarised as follows:

1) Neutrodyning can be dispensed with, which is an important advantage particularly with transmitters transmitting on different wave lengths, and in high-frequency amplification.

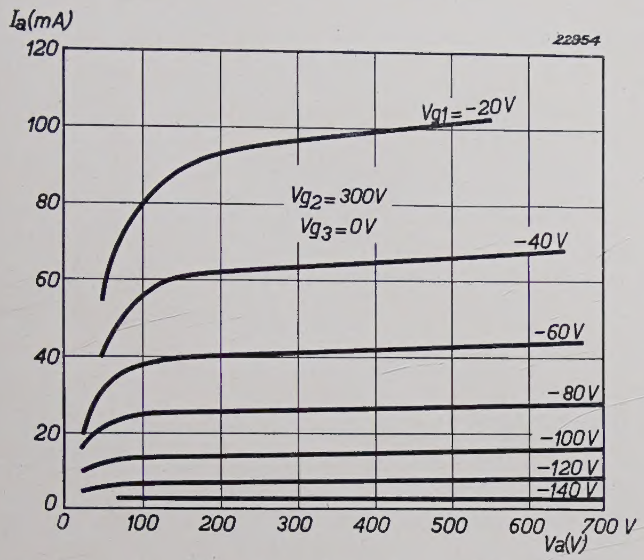

Fig. 9. Static I_a - V_a characteristic for the PE 05/15 five-electrode valve with a screen-grid voltage of 300 volts and zero suppressor-grid voltage. The anode current is independent of the anode voltage, except at very low values of this voltage.

2) Power output and efficiency are very satisfactory.

3) The excitation voltage is very small, or in other words power amplification is very high. A transmitter for a given power output therefore contains less stages when equipped with five-electrode valves than with three-electrode valves.

Use of Pentodes in Transmitters

In the use of pentodes in transmitters, a distinction may be drawn between the following applications:

a) High-frequency telegraphy amplification,
b) High-frequency telephony amplification (class B amplification),
c) Modulation of high-frequency oscillations, which are amplified by the valve.

a) When used for high-frequency amplification in telegraph circuits, the adjustment of the valve must be such that the maximum power output is obtained at the optimum efficiency. Class C conditions are therefore desirable in this case. The limits of adjustment are due to the maximum permissible dissipation in the anode and the screen grid and the maximum direct cathode current.

b) When used as a high-frequency telephony amplifier the excitation voltage is modulated on a low-frequency carrier, which means that modulation in one of the preceding stages of the transmitter is necessary. Adjustment must naturally be such that the modulation of the excitation voltage is preserved without distortion in the aerial current.

For this purpose the negative bias at the control grid must be made so large that with the screen grid voltage used the anode current is nearly zero (class B amplification).

That there is then a linear relationship between the aerial current and the amplitude of the excitation voltage may be seen from the following:

It is shown in fig. 2*b* that the anode current curve is composed of half-waves at intervals of half a cycle, i.e. the time during which the current flows is always half of a full cycle.

For a current curve of this type the ratio between the maximum current I_{a_m} and the amplitude of the first harmonic I_{a_1} is constant and equal to $^1/_2\,\pi$, it is thus independent of the value of I_{a_m}.

As the static characteristic of the valve is nearly straight I_{a_m} is proportional to $V_{g_1\sim}$, from which it follows that I_{a_1} is proportional to $V_{g_1\sim}$. From equations (1) and (2) we get furthermore:

$$P_0 = {}^1/_2\, I_{a_1}\, V_{a\sim} = {}^1/_2\, I_{a_1}^2\, R_a \quad \cdot \cdot \quad (7)$$

This power reaches the aerial, and if I_{ant} is the effective value of the aerial current and R_{ant} the aerial resistance, we have:

$$P_0 = I_{\text{ant}}^2\, R_{\text{ant}} \quad \cdot \cdot \cdot \cdot \cdot \cdot \cdot \cdot \cdot \cdot \quad (8)$$

We get from equations (7) and (8):

$$I_{\text{ant}} = I_{a_1} \sqrt{\frac{R}{2\,R_{\text{ant}}}} = \text{const.} \cdot I_{a_1}, \quad \cdot \quad (9)$$

i.e. I_{ant} is proportional to I_{a_1} and according to the above is also proportional to $V_{g_1\sim}$.

c) Finally, the high-frequency oscillation which is amplified by the valve can be modulated with a low-frequency voltage by impressing this low-frequency voltage on the direct voltage of one of the electrodes. This can be done in the following ways:

1) Anode modulation,
2) Suppressor-grid modulation,
3) Screen-grid modulation,
4) Control-grid modulation,
5) Simultaneous modulation at the anode and screen grid.

In all cases the valve is used as a class-C amplifier.

In each of these methods of modulation there must be a straight-line relationship between the aerial current and the direct voltage at the electrode

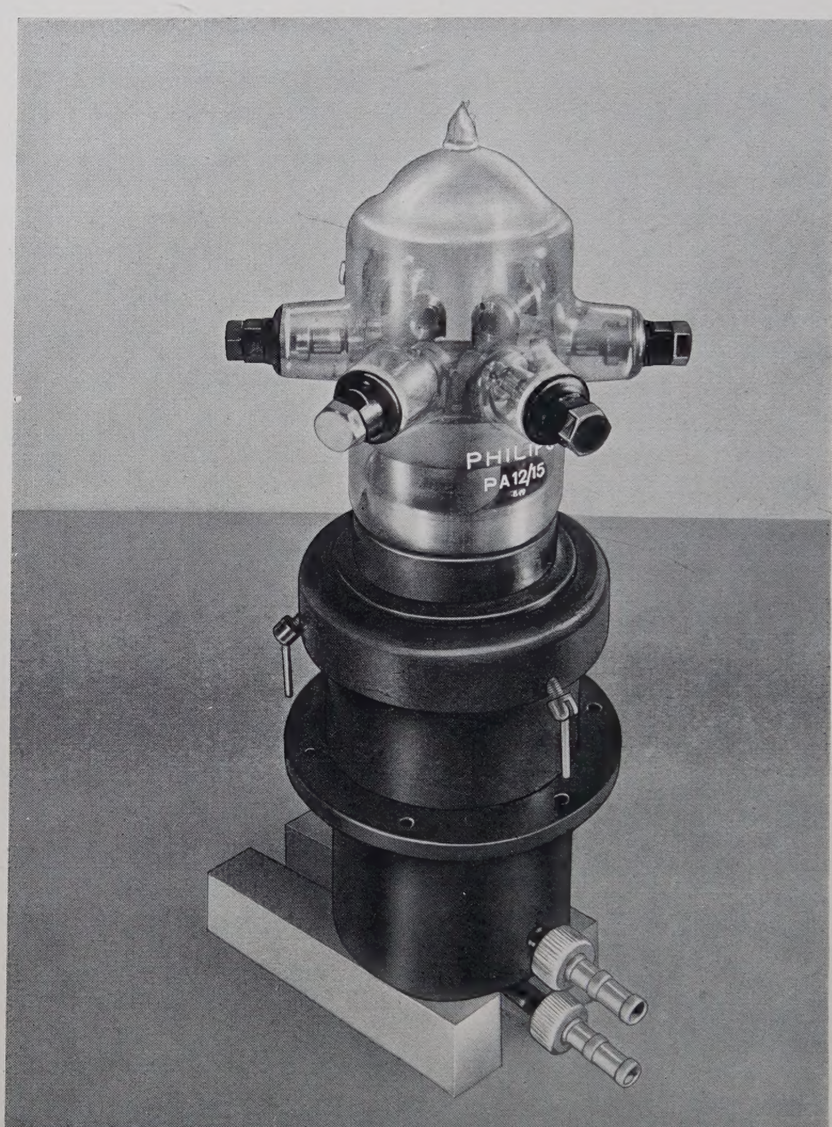

Fig. 10. The PA 12/15 five-electrode valve has a tungsten cathode and is water-cooled. It has an output exceeding 15 kilowatts and has been designed for wavelengths of about 6 m, being thus particularly suitable for short-wave radio and telephone transmitters and for television transmitters.

on which the modulation voltage is impressed, since the modulation must be reproduced without distortion. It has been found in practice that a satisfactory linear relationship is readily obtainable by methods 1), 2) and 5), but that this is difficult with 3) and 4).

In modulation at the suppressor grid, the fact is used that the anode current is the smaller the higher the negative voltage applied to the suppressor grid. This is due to the partial rejection by the negative suppressor grid of the slower electrons, so that not all the electrons reach the anode.

The relationship between the aerial current and the suppressor grid voltage has been found satisfactorily linear so that good modulation may be obtained. A particular advantage found with modulation at the suppressor grid is that no power for modulation is required, for since the suppressor grid remains negative throughout modulation no current flows to this grid. The modulator can therefore be made small even with the largest of the five-electrode valves, e.g. the PC 3/1000.

Properties of the Philips Transmitting Pentode

Philips manufacture the following five-electrode transmitting valves:
PE 05/15, OC 05/15, PC 1/50, PE 1/80, PC 1.5/100, PC 3/1000 and PA 12/15. The power outputs of these valves lie between 15 watts with the first valve over 15 kilowatts with the last valve. Of these valves PE 05/15 and PE 1/80 have indirectly-heated cathodes, PA 12/15 has a tungsten cathode and the other valves a directly-heated oxide cathode. The PA 12/15 transmitting valve is water-cooled and is shown in *fig. 10.*

It has already been seen that the control grid current in these valves is very small as compared with that in three-electrode valves, and that the excitation power also is hence much smaller.

A comparison is made in the following table between the TC 1/75 three-electrode valve and the PC 1.5/100 five-electrode valve, the data relating to the so-called telegraph adjustment, i.e. at which the valves give their highest output.

		TC 1/75	PC1.5/100
Anode voltage	V_a	1500 V	1500 V
Control-grid voltage	V_{g1}	—160 V	—200 V
Screen-grid voltage	V_{g2}	—	300 V
Suppressor-grid voltage	V_{g3}	—	0 V
Anode current	I_a	123 mA	145 mA
Control-grid current	I_{g1}	12 mA	3.5 mA
Screen-grid current	I_{g2}	—	50 mA
Excitation voltage	V_{g1}	240 V	280 V
Excitation power	P_{hf}	2.9 W	1.0 W
Anode power input	P_{ia}	185 W	218 W
Anode dissipation	P_a	70 W	77 W
Screen-grid dissipation	P_{g2}	—	15 W
High-frequency power output	P_0	115 W	141 W
Anode efficiency	η_a	62.2 %	65 %
Ratio $\frac{\text{power output}}{\text{excitation power}}$	$\frac{P_0}{P_{hf}}$	40	141
Capacity between anode and control grid	C_{ag1}	10.4 μμF	0.03 μμF

It is seen from this table that the ratio of the power output to the excitation power is 141 with the five-electrode valve and 40 with the three-electrode valve, the five-electrode valve thus having a marked advantage in this direction.

THE RELATIONSHIP BETWEEN FORTISSIMO AND PIANISSIMO

By R. VERMEULEN.

The vigour which should characterise well-reproduced music is dependent upon adequate reconstitution of the original contrasts between fortissimo and pianissimo. It is well known that acoustical contrasts in the reproduction of a musical item are less pronounced than in the original rendering.

A check is imposed on the fortissimo by the restricted output of the amplifier and the loudspeaker; this limitation is, however, not of a fundamental character, since in the present state of technology the output can always be raised to the economic level justified in each particular case. The range of the contrasts which can be reproduced is also limited by the characteristics of the transmission members, which include not only the cables and the wiring in a radio plant, by which reproduction is transmitted to a distant point, but also the gramophone disc, the sound film and the "Philimil strip" [1]) which all permit the reproduction of music at times subsequent to their actual execution. All these reproduction and transmission units possess a characteristic maximum-permissible depth of modulation being determined either by cross-talk interference from other cores in the same cables, by the carrier wave used in broadcasting, by the mutual distance between the grooves in a disc, or by the width and optical transmission properties of the sound track on the film. This maximum modulation value must reproduce the fortissimo. In this connection it should be noted that the actual intensity of the maximum signal obtained is of secondary importance, since it can be magnified to any level by amplification, and its limitation in the fortissimo direction does not therefore of itself constitute a restriction of the brilliance.

It is, however, found that in the other direction, viz., towards the pianissimi, there is also a limit of response and that it is not practicable to use arbitrary low depths of modulation. The reproduction of the pianissimi is restricted by the interference phenomena which occur with every transmission system and which are usually referred to as "mush" or background noise. These interference phenomena may be due to a variety of very different causes. They are usually of such weak intensity that at a superficial glance they appear to be negligible, yet owing to the very wide range of sound intensities which are audible to the ear, even the slightest interference noise may still be detectible. With gramophone records, the surface inequalities of microscopic dimensions are the principal source of this interference; in the sound film individual silver grains of the light-sensitive emulsion and various other particles on the film, as well as the general deterioration of the surface, which determines the amount of light transmitted, may be responsible for interference.

If the interference is very weak, but of frequent occurrence, as for instance with inequalities in the disc grooves and with grains in the light-sensitive emulsion, impulses of very short duration will be produced during reproduction and these will occur at random and with an indeterminate frequency. The ear will detect these sources of interference as "mush" of roughly constant intensity and uniform timbre without any particular pitch. The best example of this is the shot effect, which has been discussed in a previous article in this Review [2]).

With the "Philimil" strips, the intensity of this background noise is very much reduced owing to the absence of grains in the coating and the sharpness of the freshly-inscribed surface. Nevertheless a residual mush remains also with these strips. Dust particles which can never be entirely excluded become audible as a low mumbling sound and impose a new, although lower, limit to the reproduction of weak sounds.

The height of the interference level, which is taken to include all types of unwanted and spurious noises, including mush and mumbling, also determines the maximum ratio between the fortissimi and pianissimi which can be reproduced or transmitted without distortion. It has already been pointed out that this ratio is too small for the reproduction in correct proportion of all the sound intensities obtained with a large symphony orchestra. It devolves, therefore, on the engineers operating and controlling the microphone potentiometer to maintain the frequency sweep recorded between the limits imposed on efficient reproduction, but without appreciably detracting from the general effect produced. To obtain this result the usual policy adopted is to leave the crescendi and decrescendi unaltered and to regulate only very slowly in the more constant parts. From the score

[1]) See Philips techn. Rev., **1**, 107, 135, 211 and 230, 1936.

[2]) M. Ziegler: The causes of noise in amplifiers, Philips techn. Rev., **2**, 136, 1937.

those passages are located where considerable differences in sound are to be expected as well as those where regulation will not spoil the general musical effect; these passages are marked in the score.

As an example of the variety of sound intensities carefully fixed at the start and not altered in the course of each measurement. At the same time a sound track was made on a "Philimil strip" in which the amplification was adapted to the limits of modulation using the method already described.

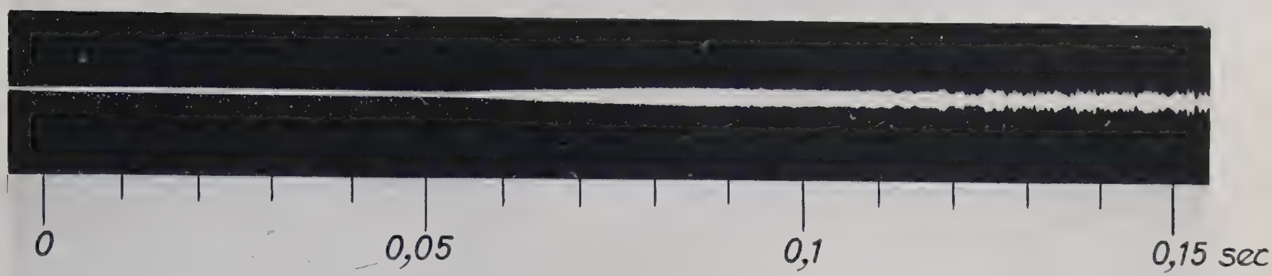

Fig. 2. Registration on the "Philimil strip" of the 160—161 bars where the sound intensity suddenly increases. This strip has been enlarged three times and the sound recorded thus covers only 0.15 of a sec. It is seen that one of the instruments started playing 0.05 sec before the others.

which normally occur, there are reproduced below records of the sound intensities registered in the auditorium of the Philips Works' Theatre at Eindhoven during a concert given by the Amsterdam

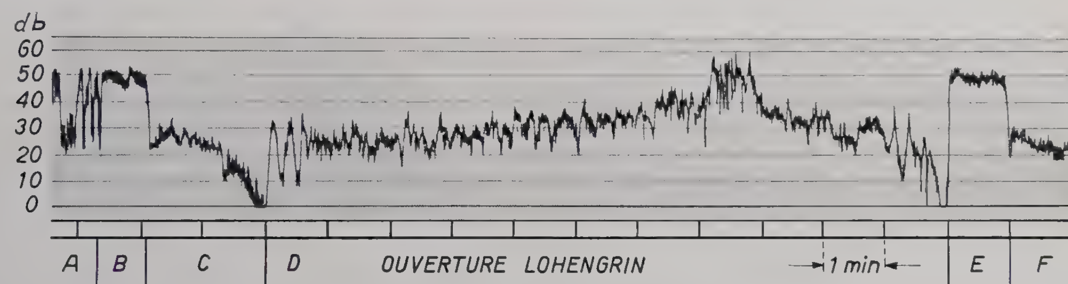

Fig. 3. Overture to Lohengrin, Richard Wagner, played by the "Concertgebouw-orkest" under the direction of Prof. Dr. Willem Mengelberg at the Philips Works' Theatre in Eindhoven. The letters denote:

A Last chord of the Eighth Symphony of Beethoven, which preceded the Overture.

B Applause. The return of the conductor is indicated by the renewed applause.

C Noises in the auditorium between the two pieces. The noises subside at the beginning of the overture.

D Registration of the Lohengrin Overture; the opening chords, the peak sound at the 54th bar and the closing chords can be clearly distinguished. The closing bars are played *pp*, only four violins playing, and the sound intensity then drops below the threshold of registration of the recorder. The range of sound intensities thus exceeded 60 decibels.

E Applause lasting 1 minute.

E Noises in the auditorium during the interval. As the audience left the auditorium during the interval these noises gradually subsided.

"Concertgebouworkest" under the direction of Prof. Dr. Willem Mengelberg. To record these sounds, they were picked up by a microphone and the microphone voltage measured, after amplification, by means of a recording voltmeter with logarithmic scale. The amplification was naturally

Fig. 1 reproduces the record made of the opening bars of the first part of the Sixth Symphony of Tschaikowsky, Opus 74. The top strip is the record made in the auditorium itself. The beginning of the record at a level of 35 decibels represents the noise in the auditorium at the end of the interval; this noise gradually subsided as the audience took their seats. The conductor on entering was greeted with applause of 55 decibels intensity for a period of 15 secs. The noise in the auditorium

then quickly subsided, a few sharp peaks being however produced by coughing in the audience. The adagio was played by the bass-viols only, and which played *pp*; the bassoons then came in with the theme playing loud crescendi and diminuendi of nearly 15 decibels. It is not proposed to discuss in this article the rendering of each bar of the symphony, but for the guidance of those interested

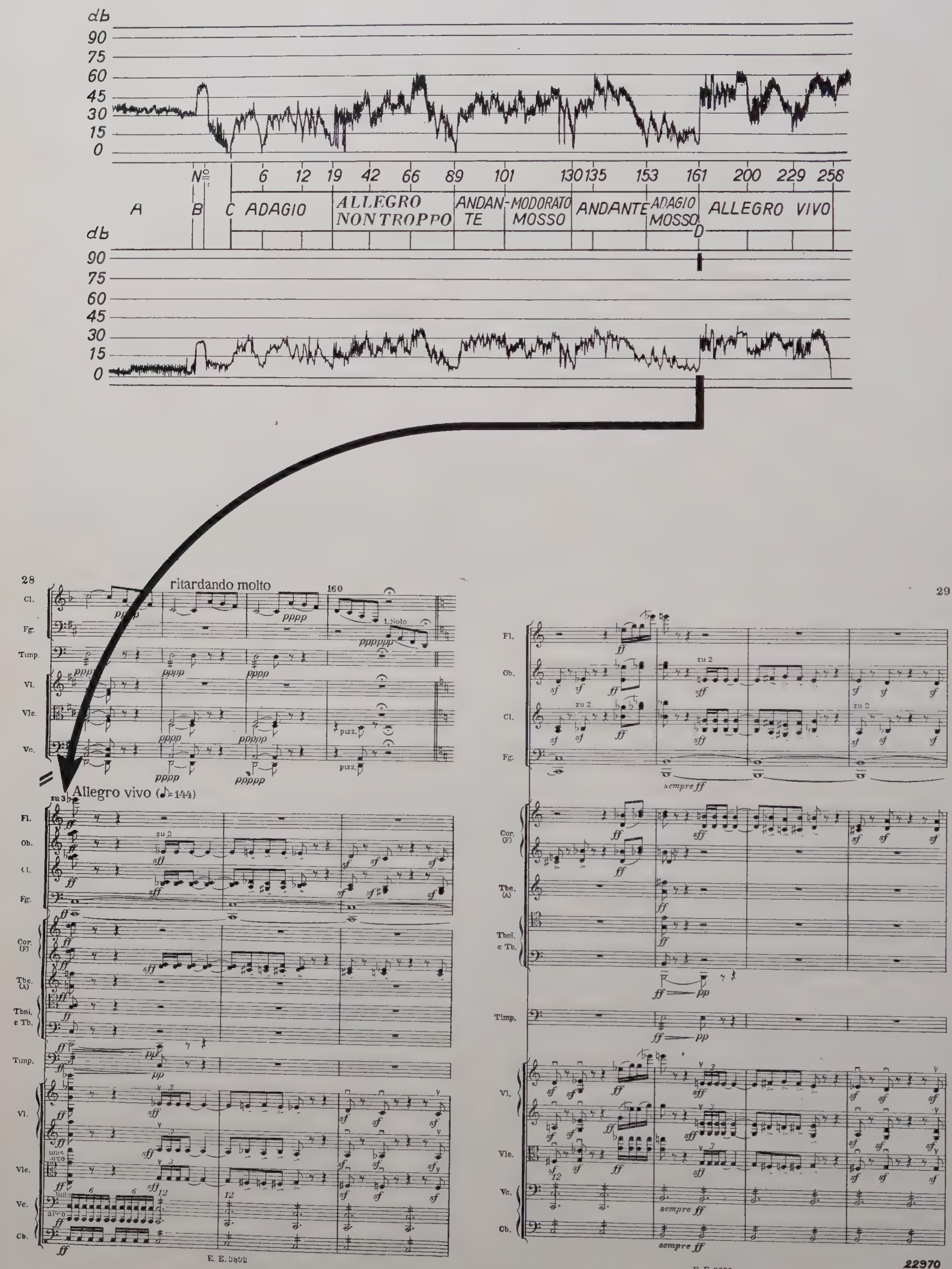

Fig. 1. Explanation at the bottom of page 269.

and who have a score of this symphony available, the times of certain characteristic passages are indicated below the audiogram. The sharpest contrast is obtained at the *ff* start of the allegro vivo passage at the 161st bar following an organ point (a prolonged muted tone) of the first bassoon marked *pppppp* in the score. The difference in the sound intensities is 45 decibels; to illustrate this more clearly the corresponding page from the score has been printed below the sound records, with this difficult point marked with an arrow and two strokes. A section of the "Philimil" strip with the sound track of this passage is shown enlarged three times in *fig. 2*.

Under the sound-intensity record made in the auditorium, the record is reproduced of the voltage delivered by the photocell amplifier of the Philips Miller reproduction apparatus and which was registered on the following day. This record shows the effect of potentiometer regulation, and it is evident that the difference between the maximum and minimum sound intensities has been reduced, and that in particular the extreme maxima have been lowered and the minima not allowed to drop to the previous level as these are always limited by the interference level. The start of the record shows the background noise of the "Philimil strip", although after half a minute the potentiometer was stepped up and the noise in the auditorium recorded at a lower level. Just before the applause greeting the conductor, the potentiometer was stepped down in order to deal with the contrast in sound of the applause. During the interval of comparative quiet before the symphony commenced the amplification was again increased, and so on. It may be concluded from the measurements that the difference in sound intensity was about 55 decibels; to arrive at this figure the points at which the orchestra was not playing (e.g. bar 6 and bar 89) must naturally not be included. On the "Philimil strip" this difference has been reduced to 38 decibels, during which the extreme limits of modulation were not reached at any point in order to maintain the efficiency of registration.

Fig. 3 shows another registration made during the same concert, which included the overture to Lohengrin by Richard Wagner. Further details of this sound record are given in the caption under fig. 3.

It is interesting to note that, in spite of the successive crescendi and decrescendi, the intensity level on the average gradually increased, reached a maximum and then gradually diminished again.

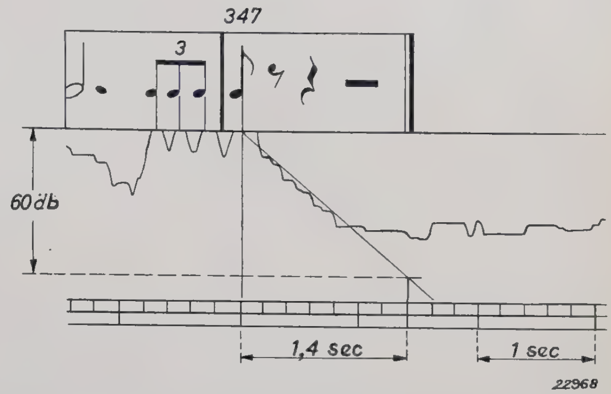

Fig. 4. Reverberation measurement. The time scale in this diagram is about 12 times greater than that used in fig. 3. Registration was made during the closing bars of the third part of the Sixth Symphony of Tschaikowsky. At the top edge, the sound intensity exceeded the range of the apparatus. The individual sounds can be clearly distinguished; the actual notes of these two bars are shown at the top of the figure.
After the closing chord the sound in the auditorium decayed to the prevailing noise level. Although there are irregularities in the course of the curve due to interference caused by various reflections, a mean line can easily be drawn. This line indicates that the rate of decay of the sound was 60 decibels in 1.4 sec, so that the mean time of reverberation of the auditorium was 1.4 sec.

Fig. 4 shows with a highly-magnified time scale a few bars from the end of the third part of the Sixth Symphony of Tschaikowsky already referred to. The orchestra finished this passage sharply with a fortissimo, after which the sound gradually died away by reverberation in the auditorium. In this way [3]) the mean reverberation in a full auditorium can be measured without distracting the audience with whistles or other obnoxious sounds.

[3]) This method was first used by E. Meyer and V. Jordan, E.N.T., **12**, 213, 1935.

Fig. 1. Sixth Symphony part 1, P. Tschaikowsky, Opus 74, played by the Concertgebouworkest under the direction of Prof. Dr. Willem Mengelberg in the Philips Works' Theatre at Eindhoven. The axis of reference of the registered waves has been arbitrarily chosen so that only differences in sound intensity should be read off; the absolute sound level is unknown.

The same time scale is used as in fig. 3, viz., 8 mm = 1 min.

The upper strip is the record of the sound intensity in the auditorium. The figures given under this record are the numbers of the bars at characteristic points. The letters below the numbers represent:

A Noise in auditorium during the interval.

B Applause as the conductor enters.

C Beginning of orchestral music.

D Start of allegro vivo passage which has its greatest contrasts.

The times of its various passages are also given. The lower strip is the record of the same bars when reproduced with the Philips Miller apparatus. Below is the score in which the arrow points to the place corresponding to *D* in the records.

A SIMPLE ELECTRICAL MEASURING BRIDGE

Summary. In this article are described the arrangement and applications of a simple electrical measuring bridge designed for an alternating current supply, the "Philoscop, type G.M. 4140". The indicator consists of a five-electrode valve with a simple form of cathode-ray tube or "electron-ray" tuning indicator. With this bridge, resistances from 0.1 ohm to 10 megohms and capacities from 1 $\mu\mu$F to 10 μF, as well as self-inductances and composite impedances, can be measured. The apparatus is also suitable for other purposes, such as the tracing of interference, the testing of faulty insulation and for the measurement of low voltages.

Introduction

A simple measuring apparatus enabling rapid and reasonably accurate measurements of resistances, capacities and self-inductances to be made is frequently required in electrical work. The apparatus described in this article is a Wheatstone bridge designed for direct connection to an A.C. mains supply and suitable for the direct measurement of resistances between 0.1 ohm and 10 megohms and of capacities between 1 $\mu\mu$F and 10 μF. The ratio between the highest and lowest values which can be measured with this apparatus is $10^8 : 1$ in the case of resistances and $10^7 : 1$ with capacities. Furthermore by connecting suitable external resistance, capacity and self-inductance standards or combinations of these to the bridge, a large number of comparative measurements can be made on the basis of a bridge circuit.

In designing this apparatus, greater importance was attached to obtaining the widest possible range of applications for the bridge, than to a high degree of accuracy. The average accuracy with direct readings is just over one per cent, while for the comparative measurements referred to it is one per thousand. This relatively low accuracy is, however, adequately made up for by the rapidity with which measurements can be carried out, both in the high and low ranges, and by the fact that the apparatus does not require a battery as it is fed directly from the mains.

Sensitivity of the Measuring Bridge

One of the most interesting components of the apparatus is the indicating arrangement, which has a very high impedance and thus absorbs practically no current. In consequence, the "sensitivity" of measurement, i.e. the deflection of the instrument when the contact on the slide wire is displaced by a definite amount from the position of balance, is independent of the magnitude of the resistance under measurement. Usually the resistance of the indicating galvanometer is not higher than the bridge resistances, so that the sensitivity of measurement decreases rapidly as the resistance values increase.

This may be explained more clearly with the aid of the fundamental circuit of the Wheatstone bridge shown in *fig. 1*. If the difference in potential

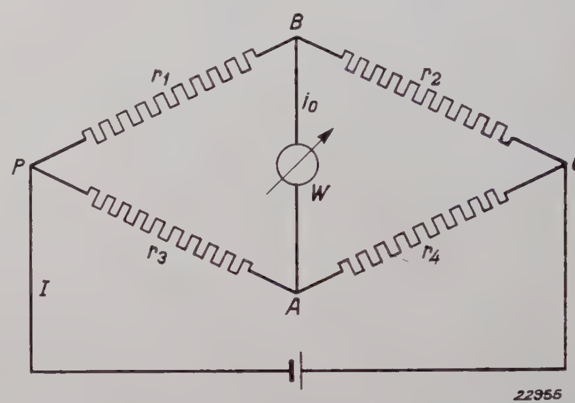

Fig. 1. Fundamental circuit of the Wheatstone bridge. $r_1 \ldots r_4$ are the bridge resistances. w is the resistance of the galvanometer circuit.

between P and Q is equal to V_P-V_Q, then from Kirchhoff's laws, according to which the algebraic sum of the current intensities meeting at any point of a conducting network is zero and also in each closed circuit the algebraic sum of the products of the currents and the resistances is equal to the sum of the electromotive forces, we can calculate that:

$$V_A - V_B = \frac{(V_P - V_Q)\, w\, (r_2 r_3 - r_1 r_4)}{w\,(r_1 + r_2)(r_3 + r_4) + r_1 r_2 (r_3 + r_4) + r_3 r_4 (r_1 + r_2)} .$$

The bridge is balanced, when $r_2 r_3 - r_1 r_4 = 0$; the difference in potential $V_A - V_B$ is then zero. In most cases, and also in the present apparatus, two of the bridge resistances, which are connected in series, e.g. r_1 and r_2, are made in the form of a slide wire. Their sum is therefore constant, but by displacing the point of contact B along the wire their ratio can be altered, until $V_A - V_B = 0$. r_4 is then the resistance required and r_3 the known resistance, and in the balanced condition we have:

$$r_4 = r_3 \cdot \frac{r_2}{r_1} .$$

If the bridge is brought out of balance, for instance by increasing r_1 by a small amount Δr, which at the same time decreases r_2 by Δr, the alteration in potential between A and B will be:

$$\Delta (V_A - V_B) = -\frac{(V_P - V_Q)\,\Delta r}{r_1 + r_2} \cdot \frac{1}{1 + \frac{r_1 r_2}{r_1 + r_2} \cdot \frac{1}{w} + \frac{r_3 r_4}{r_3 + r_4} \cdot \frac{1}{w}}.$$

The resistance of the slide wire $r_1 + r_2$ is usually small compared with the resistance w of the galvanometer which is used to indicate when the bridge current is zero. Most modern galvanometers are moving-coil instruments with a resistance not exceeding 1000 ohms, the resistance of the slide wire is usually however much lower, so that $\frac{r_1 r_2}{w\,(r_1 + r_2)}$ is small and may be neglected compared with unity. It is evident that the other term in the denominator $\frac{r_3 r_4}{(r_3 + r_4)\,w}$ can not be neglected, especially when measuring high resistances, as it determines the sensitivity in these measurements.

The instrument however used in the bridge described here has a *very high* resistance w, in fact higher than the maximum resistance to be measured: $\Delta (V_A - V_B)$, which is proportional to the reading obtained is hence:

$$\Delta (V_A - V_B) = -\frac{(V_P - V_Q)\,\Delta r}{r_1 + r_2},$$

and is therefore constant and independent of the value of the resistance under measurement. This high resistance, in conjunction with an adequate voltage sensitivity of the galvanometer, has been realised by connecting the points A and B to the cathode and the grid of an amplifying valve, as will be described in more detail when dealing with the indicating component.

The Bridge

If resistance of 0.1 ohm and 10^6 ohms are measured with the same bridge incorporating a single standard resistance of, for example, 1000 ohms, by merely altering the slide-wire ratio, this ratio will be small for 0.1 ohm and high for 10^6 ohms. These maximum and minimum ratios are, however, not accurately ascertainable, because at a given absolute accuracy in reading for both arms of the slide wire the percentage accuracy with which the smaller arm can be ascertained is much less than that in the case of the longer arm. A ratio which is either too high or too low is therefore undesirable. In practice the slide wire is used only for ratios between 0.1 and 10. This limitation in the ratio is obtained by connecting in series with each end of the slide wire, which in this case has a resistance of 1000 ohms, a resistance R which restricts the range of adjustment. This arrangement is shown diagrammatically in *fig. 2*. The resistance $r_1 + r_2$

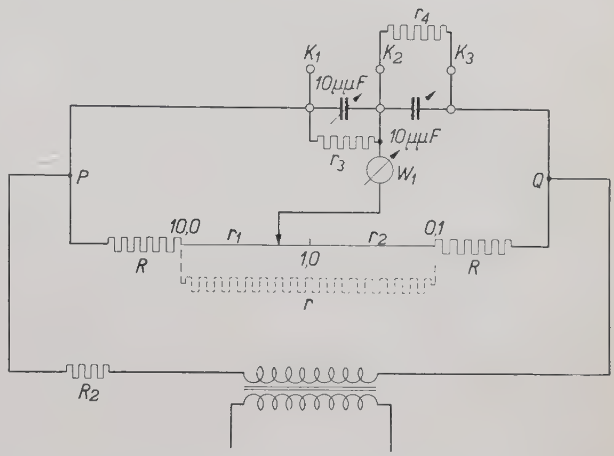

Fig. 2. Arrangement of the bridge with a slide wire in place of the resistances r_1 and r_2. The unknown resistances are connected across K_2 und K_3. The two resistances R in series with the slide wire limit the ratio between the arms of the slide wire to a range from 0.1 to 10. If r is shunted across the slide wire, this range can be reduced to form 0.8 to 1.25 (percentage scale), thus raising the accuracy. The variable capacities between K_1 - K_2 and K_2 - K_3 are used for adjusting the capacity of the wiring to 10 $\mu\mu$F. The transformator winding for feeding the bridge and the series resistance R_2 for protecting the winding also are shown.

of the slide wire and the series resistances R have such ratings that $\frac{R}{r_1 + r_2 + R} = 0.1$. It is thus not possible to measure resistance below 0.1 r_3 or above 10 r_3. Four resistances have therefore been incorporated in the bridge for r_3, which differ from each other in steps of 100. In this way, the interval from 0.1 ohm to 10 megohms is covered by four measuring ranges. The knob A_1 (*fig. 3*), which can be turned into ten different positions, is used for changing from one measuring range to another: four of these settings are used for the measurement of resistances (*fig. 4*). The position of the contact on the slide wire is adjusted and read off on the outer circumference of the circular scale R_1 (fig. 3), for which purpose the scale circle has been subdivided from 0.1 to 10, with the point 1 at which $r_1 = r_2$ situated at the centre. The division of the scale allows a direct reading of the ratio $(r_1 + R) : (r_2 + R)$.

It is evident from the above that a higher accuracy can be obtained if the ratio $(r_1 + R) : (r_2 + R)$ is

not extended over a range from 0.1 to 10, but is restricted to a narrower range. This may be done by a resistance r which is shunted across the slide wire in a particular setting of the knob A_1. This

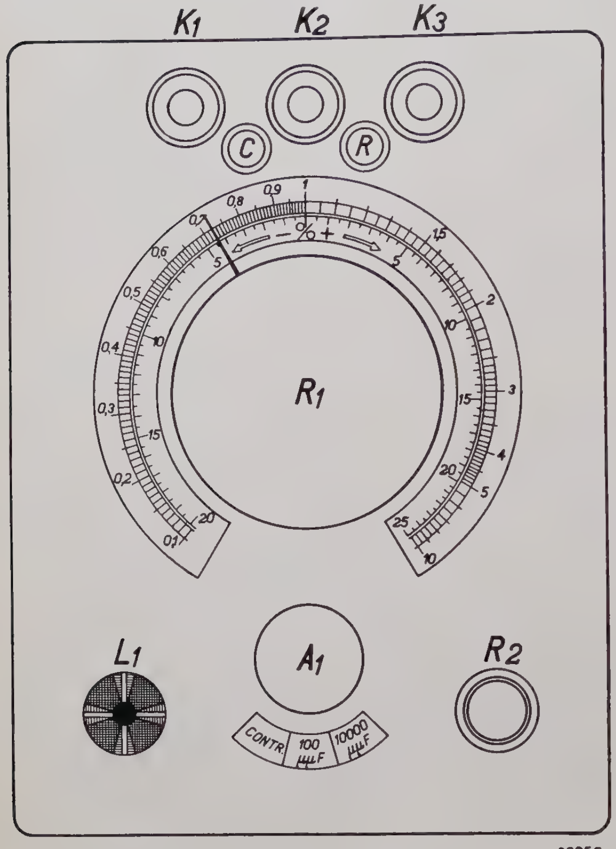

Fig. 3. Plan of apparatus. R_1 has a percentage scale and a decimal scale from 0.1 to 10, as shown. The knob A_1 serves for selection of ten different bridge settings (see also fig. 4). The "electron ray" indicator L_1 is viewed through a window. R_2 regulates the sensitivity by means of the grid leak of the "electron ray" indicator, K_1, K_2 und K_3 are terminals for connecting the resistances R and the capacities C. The earth terminal is not visible being on one of the sides.

resistance shunt is shown by broken lines in fig. 2. The resistance $\frac{(r_1 + r_2)\, r}{r_1 + r_2 + r} < r_1 + r_2$ is then connected across the ends of the slide wire between which regulation is possible. The resistance r is so adjusted that a complete rotation of the knob R_1 over the scale corresponds to a range of ratios from 0.8 to 1.25.

This higher degree of accuracy is used for measuring the percentage deviation of a resistance from a standard of nearly the same value. The corresponding percentage scale is marked along the inner circumference of the circular scale (see fig. 3). In this arrangement the bridge contains no standard resistance, so that this together with the unknown resistance, has to be connected up externally. This setting is termed the "open bridge" setting.

In another position of A_1 two exactly equal resistances are connected to the bridge in place of r_3 and r_4. In this test setting, R_1 should read 1.0 when the bridge is balanced. If this is not the case,

Fig. 4. Scale A_1, which turns together with its knob.

the adjustment can be corrected by slightly displacing the knob R_1 on its spindle. Readjustment of the bridge is, however, rarely necessary.

Since the bridge is connected to an A.C. supply, it is also suitable for *capacity measurements*, when r_3 and r_4 are replaced by capacities C_3 and C_4, The impedance of a capacity C is $1/j\,\omega\;C$ and the condition of balance of the bridge when using resistances: $r_2\, r_3 - r_1\, r_4 = 0$ then becomes $r_2\, C_3 - r_1\, C_3 = 0$ or $C_3 = r_2/r_1\; C_4$. To enable the same scale to be used as with resistance measurements, the standard capacity is connected up in place of the unknown resistance and *vice versa*.

For capacity measurements, the knob A_1 has three further positions for connecting up, as required, one of three capacities with ratios of $1 : 10^2 : 10^4$ to the bridge in place of r_4. The unknown capacity is connected to the bridge at two terminals which link up with a point in the bridge to which r_3 was connected in resistance measurements.

If the capacity under measurement C_3 is not a pure capacity, the currents flowing through C_3 and C_4 will not be in phase, which is in fact usually the case. The phase displacement of the voltage against the current is not strictly equal to —90 deg with condensers owing to dielectric losses, and in resistances is not usually exactly zero owing to their capacity or self-inductance. The condition $r_2\, C_4 - r_1\; C_3 = 0$ is then alone not sufficient; a second condition must also be fulfilled, viz., $\varphi_1 - \varphi_2 = \varphi_3 - \varphi_4$ between the phase angles of the four branches of the A.C. bridge, where φ_1 and φ_2 are the phase angles of r_1 and r_2, and φ_3 and φ_4 those of C_3 and C_4.

This result is readily obtained by writing:

$$r_1 = r_{10}\, e^{-i\varphi_1};\ r_2 = r_{20}\, e^{-i\varphi_2};\ r_3 = r_{30}\, e^{-i\varphi_3}$$
$$\text{and } r_4 = r_{40}\, e^{-i\varphi_4};$$

where $r_{10} \dots r_{40}$ are the moduli of $r_1 \dots r_4$ and $\varphi \dots \varphi_4$ are the phase angles. The condition of balance of the bridge $r_1 r_4 - r_2 r_3$ or

$$r_{10}\, r_{40}\, e^{-i(\varphi_1+\varphi_4)} = r_{20}\, r_{30}\, e^{-i(\varphi_2+\varphi_3)},$$

is then satisfied when:

$$r_{10}\, r_{40} - r_{20}\, r_{30} = 0$$
$$\text{and } \varphi_1 - \varphi_2 = \varphi_3 - \varphi_4.$$

Still another difference occurs between resistance and capacity measurements, due to the capacity of the bridge wiring. This capacity, which during measurements is in parallel with the standard and the unknown capacities, is adjusted to 10 $\mu\mu$F by small regulating condensers inserted between the terminals. The capacity of the wiring must be taken into account when calibrating the standard capacity and 10 $\mu\mu$F always be subtracted from the result obtained.

The capacity of the wiring is employed to useful purpose in measuring small capacities between 0 and 90 $\mu\mu$F. In the open bridge setting referred to above, R_1 is adjusted to the point 1 on the R_1 scale when no resistances are connected to the bridge The load on the two arms is then 10 $\mu\mu$F. An unknown condenser C_x will then give a value of 10 $\mu\mu$F + C_x when measuring for C_3. The limits between which C_x can be measured are determined by the condition: 10 $\mu\mu\text{F} < 10\ \mu\mu\text{F} + C_x < 100\ \mu\mu$F. The range between 0 and 90 $\mu\mu$F obtained in this way thus covers only the right half of the scale.

The Indicating Instrument

The indicating instrument constitutes the principal difference between the measuring apparatus described here and other standard types of Wheatstone bridge. As stated above, an amplifying valve, viz., the five-electrode valve EF 6 (L_2 in *fig.* 5), is used here in place of the usual galvanometer or telephone. The amplified voltage is indicated by the electron ray tuning indicator L_1. The bridge voltage between A and B in fig. 1 is applied across the cathode and the first grid of the penthode. The indicating instrument is thus made up of the penthode and the tuning indicator. The input impedance of the penthode is hence incorporated in the bridge, and is given by:

$$C_g = C_{kg} + C_{ag} \cdot \frac{gR_u}{R_i + R_u};$$

where R_i and R_u are the internal and external resistances of the five-electrode valve, g is the amplification factor, and C_{kg} and C_{ag} are the grid-cathode and the grid-anode capacities respectively.

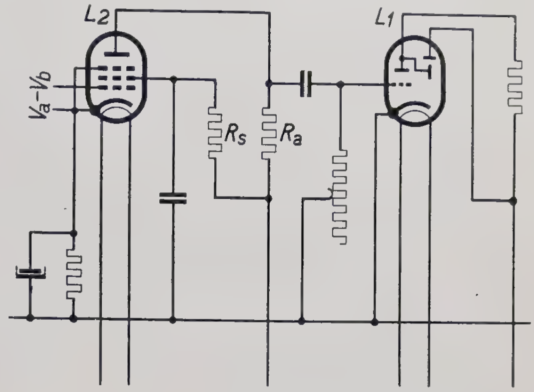

Fig. 5. Circuit diagram of the electron ray indicator L_1 with the pentode L_2, which acts as an amplifier. The bridge potential across A and B (see fig. 1) is connected to V_a- V_b. R_s supplies the screen grid voltage for the five-electrode valve. R_a is the anode resistance in the anode circuit of the five-electrode valve.

Thus C_g is approximately 5 $\mu\mu$F and $1/\omega C_g$ over 10^8 ohms at mains frequency. It can thus be claimed that the instrument has an adequately high internal resistance which satisfies the conditions set forth above.

Resistances with a blocking condenser are used for coupling the pentode and the tuning indicator in the usual way. The characteristics and method of operation of the tuning indicator are described in detail below.

In this valve a vertical, indirectly-heated cathode (*fig.* 6) emits electrons. The intensity of the electron stream can be controlled by a grid in the usual way, which in this design of valve surrounds only the lower part of the cathode. That part of the current which can be regulated in this way strikes an anode of the same length as the grid and assembled concentrically with the latter. A resistance of 2 megohms is connected to the anode, a constant voltage being applied across valve and resistance. A change in the p.d. between the cathode and grid therefore alters the voltage drop across this resistance.

The top of the cathode is surrounded by a second anode shaped like the generating surface of an inverted conical frustrum. The cone is co-axial with the cathode. From above a view is obtained of the inner surface of the cone, which is coated with a material which fluoresces under the impact of the electrons. The cone is joined directly to the anode voltage supply. In the field between the cathode and the cone, four vertical wires are arranged

symmetrically and parallel to the cathode; two of these wires (B) are shown in fig. 6. They are connected to the anode a inside the valve, and when a voltage is applied to them, produce a controllable variation of the field distribution between the cathode and the conical frustrum.

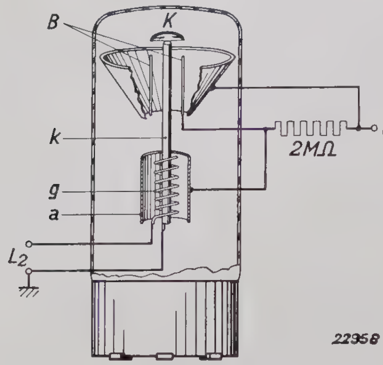

Fig. 6. Diagrammatic sketch of the electron ray tuning indicator. k is the common cathode for the three-electrode component (below) and the indicator component (at the top). a and g - Anode and grid of the three-electrode component. L_2 - Connection of five-electrode valve. B - Wires whose potential modifies the field distribution between the cathode and the cone. The luminous cross is produced by fluorescence on the inner side of the cone. K - Cap for screening the direct cathode light. The four wires B, of which one pair only is shown, are connected inside the tube to a, the anode of the three-electrode component. The voltage drop accross the 2-megohm resistance determines the voltage applied to the wires B.

If now, by altering the bridge voltage which is amplified by L_2 the potential difference between the cathode and the grid is altered, the resulting change in anode current in the lower system will produce a variable voltage drop in the 2-megohm resistance. This will alter the voltage applied to the vertical wires, so that the arms of the luminous cross, which is produced on the inner side of the cone by the modification of the field due to the vertical wires, will become broader or narrower. A variable broadening and constriction is thus superposed on the mean width at the mains frequency, but these rapid changes cannot be followed by the eye, so that the maximum width of the luminous arms is all that is visible. This maximum width, which subtends an angle Θ represents the reading of the tuning indicator. If no voltage is applied to the pentode, this angle will be a minimum. Adjustment is therefore always made to the minimum width in all cases in which the voltage has to be balanced to zero. The grid resistance of the indicator is controllable, and this alows the sensitivity, i.e. the variation of the angle Θ, to be regulated for a given change in bridge voltage.

Current Supply

A transformer of the usual type, which has separate secondary windings, furnishes the current necessary for the bridge, the anode voltages and the requisite heating voltage for the cathodes of the pentode, the tuning indicator and the rectifiers, the latter furnishing the anode voltage by double-wave rectification. A tapping is provided at the centre of the anode winding, while a filter circuit smoothes the anode voltage. A resistance in the cathode lead ensures that the grid of the five-electrode valve has an adequate negative bias with reference to the cathode. The bridge is supplied with 2 volts, applied through a resistance to protect the transformer windings in case of a short of the bridge.

The supply transformer can be changed over to one of two voltage ranges: 100—150 volts and 170—230 volts. Although the apparatus is designed principally for mains connection, the transformer can be used over a frequency range of 40 to 10 000 c/s.

Procedure of Measurements

A variety of measurements can be made with the apparatus described here and shown in *fig. 7*. The simplest measurements are those on resistances between 0.1 ohm and 10 megohms and on capacities between 1 μμF and 10 μF. In both cases the required measuring range is selected with the switch A_1, by means of which the requisite comparison resistances and capacities can be connected to the bridge. After adjusting to the value corresponding most nearly to the value under measurement, the indicator is adjusted to the minimum width by means of the knob R_1. The product of the readings

Fig. 7. General view of the bridge.

R_1 and A_1 is the value required. To maintain this simple proportionality with both resistances and capacities, the unknown resistance is connected across K_1 and K_2 and the unknown capacity across K_2 and K_3. In capacity measurements, 10 $\mu\mu$F for the wiring must then be subtracted from the reading made.

Frequently, the resistances under measurement are subject to certain tolerances, and it is useful to express the difference between a resistance, capacity or self-inductance conforming with certain specifications, as a percentage of the rating of another component of the same design. These measurements are provided for by the percentage scale of R_1. A_1 is then turned to setting $^0/_0$, and with this open bridge setting in which the resistance r is in parallel with the slide wire, the standard resistance, capacity or self-inductance is connected across K_1 and K_2 and the unknown component across K_2 and K_3. The bridge is then balanced with the aid of R_1, and differences from —20 to +25 per cent can be directly read off on the percentage scale.

With the knob A_1 in position *1*, a resistance, capacity or self-inductance can be similarly measured within a range of $1/10\,x$ and $10\,x$ when using an external standard x. This position of A_1 also corresponds to an open bridge, but in which no resistance is shunted across the slide wire. The standard and unknown component are again connected across K_1 - K_2 and K_2 - K_3. The value of the standard multiplied by the reading on R_1 at which the bridge is balanced is the required impedance.

The various settings of the bridge obtained with A_1 give the following measuring circuits:

1) Open bridge; ratio between the two arms of the slide wire is variable from 0.1 to 10. Comparison standards and unknown components are connected externally.

2) Open bridge ($^0/_0$), with increased sensitivity, i.e. the ratio range of the two arms of the slide wire is reduced to 0.8 to 1.25; percentage scale; external connection of the comparison standard and the unknown component.

3) Testing position for readjustment of the bridge.

4,5 and 6) Capacity measurements with three capacities from 10 $\mu\mu$F to 10 μF incorporated in the bridge. The capacity under measurement is connected externally.

7, 8, 9 and 10) Resistance measurements with four resistances incorporated in the bridge. Four-stage measuring range from 0.1 ohm to 10 megohms. The resistance under measurement is connected externally.

The amplifier with tuning indicator incorporated in the apparatus can also be used as a separate

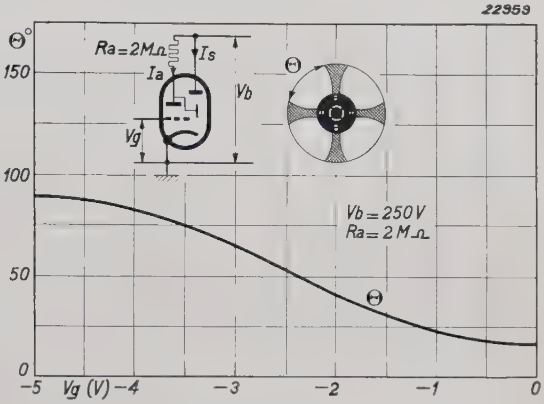

Fig. 8. Angle Θ between two arms of the luminous cross plotted against V_g between the cathode and grid of the three-electrode component of the tuning indicator. The maximum sensitivity is 25 degrees per volt. With a 2000-fold amplification in the five-electrode valve, the sensitivity of the combination L_1 and L_2 is 0.02 millivolt per degree.

voltage indicator. For this measurement the two points whose difference in potential is to be measured are connected across K_2 and the earth terminal. The broadening of the cathode ray tuning indicator is then a measure of the applied voltage. Similarly the apparatus can be used for the location of interference sources, while the output voltage of amplifiers or radio receivers can also be measured. In *fig. 8* the grid voltage of the tuning indicator is plotted against the angle Θ between the boundaries of the electron star, when the instrument is used for this purpose.

Contributed by P. G. CATH.

EQUIVALENT NETWORKS WITH HIGHLY-SATURATED IRON CORES WITH SPECIAL REFERENCE TO THEIR USE IN THE DESIGN OF STABILISERS [1])

By H. A. W. KLINKHAMER.

Summary. A design method is evolved which enables electrical equipment to be designed whose action depends on the characteristic shape of the *BH* curve of the iron in a choke coil or in a transformer with a closed magnetic circuit, without the need for complex calculations or making a large number of experimental models.

A characteristic or an oscillograph record obtained with a single specimen of the type of unit in question is shown to apply to similar designs but based on different scale, and such curve can, therefore, furnish valuable data of the properties of a large number of other designs.

A general proof of the theorem is given on the basis of arbitrary networks which contain, apart from the transformer referred to above, only constant magnitudes (resistances, capacities, self and mutual inductance coefficients, and constants of rotating commutator motors and amplifying valves). The network may also contain rectifying valves. The conditions of operation of large electrical equipment can, therefore, be studied on small-scale specimens, so that a single testing equipment can with advantage be devised for this purpose with which the most varied types of designs can be investigated.

To illustrate the general analysis of the problem, a stabliser for compensating fluctuations in mains voltage is discussed. A number of formulae are deduced for this device in which only the values of the required input and output voltages and the current intensity have to be substituted in order to obtain all the constructional data necessary.

Introduction

Devices whose action depends on the deviations from linearity in the relationship between the magnetic induction B and the field intensity H of iron have been used for a great variety of purposes from the very beginnings of electrical engineering and, in fact, form the subject of a large number of patents. Arrangements for frequency conversion and for controlling choking coils by means of initial magnetisation with direct current, and stabilisers for compensating fluctuations in mains voltage are but a few typical examples of the many devices in this group. There can be little doubt that these devices would be in more general employment if their use were not hampered by two difficulties:

Firstly, little definite information is usually available of the form of the *BH* curve, for the standard delivery specifications relating to transformer and dynamo sheets require only one and at most two points on this curve to be given and then only in reference to the lower limit.

Secondly, advance calculations are very difficult. Since sinusoidal currents are not under consideration, A.C. vectors can only be employed to give a rough approximation. Moreover, the actual performance frequently differs from that previously deduced theoretically by means of A.C. vector analysis. Analysis fails to provide a more accurate treatment applicable to practical conditions, in spite of many attempts which have been made in this direction.

The first difficulty may be overcome by the determination of the characteristics of each piece of equipment separately, for instance by altering the height of the core, although this method is impracticable for mass production. Moreover, the equipment then acquires larger dimensions and is more costly to construct, since in every direction the unfavourable deviation of the *BH* curve has to be taken into consideration.

The second difficulty need not hamper the manufacturer, for to draft a design of a particular piece of equipment it is by no means necessary to make a large number of complex calculations; a design can be based entirely on the results of direct measurement, without having to build a series of experimental models of the particular equipment to be designed.

How this can be done forms the subject of the present article.

Equivalent Designs

To analyse the problem generally, consider an arbitrary network of which one branch contains a choke coil with a closed iron core. We will limit

[1]) This article is a summary of the contribution of the author: "Over het ontwerpen van inrichtingen met verzadigde ijzerkern" to the Prof. Feldmann memorial volume: Electrotechnische Opstellen (Waltman, Delft, 1937).

our discussion to cores of a shape where the cross-sectional area of the core is the same throughout the magnetic circuit.

Let the various constants of the network be as follows:

N Number of turns on the core.
l Length of iron circuit.
F Cross-sectional area of iron.
R, L, C Resistance, self-inductance and capacity.

Let the variables of the network be as follows:

t Time.
Q Charge or quantity of electricity passed.
$I = dQ/dt$, current, for $t = 0$, $Q = Q_0$ and $I = I_0$.
U External e.m.f.
E Reactive e.m.f. of the elements forming the network.
B Inductance of the iron core.
H Field intensity of the core.

Starting from given initial conditions such as:

$$Q = Q_0 \text{ and } I = I_0$$

the values of the variables will be determined completely by the following set of equations:

For every branch except that containing an iron choke coil

$$U = U(t), \quad (1)$$

$$I = \frac{dQ}{dt}, \quad (2)$$

$$-E = L\frac{dI}{dt} + RI + \frac{Q}{C}. \quad (3)$$

For the iron-cored circuit

$$-E = NF\frac{dB}{dt}, \quad (4)$$

$$4\pi N I = H l, \quad (5)$$

$$B = f(H), \quad (6)$$

For each mesh $\Sigma(E + U) = 0$, (7)

For each junction point $\Sigma I = 0$ (8)

The function f in equation (6) is determined by the BH curve of the material of the core, which may be assumed to be known. The functions $U(t)$ which represent the external e.m.f.'s in terms of the time are also known.

Make the following substitutions in equations (1) to (8):

$$t = \frac{1}{k}t', \quad (9)$$

$$E = k\frac{F N}{F'N'}E', \quad (10)$$

$$U = k\frac{F N}{F'N'}U', \quad (11)$$

$$Q = \frac{1}{k}\frac{N' l}{N l'}Q', \quad (12)$$

$$I = \frac{N' l}{N l'}I', \quad (13)$$

$$L = \frac{F l'}{F' l}\left(\frac{N}{N'}\right)^2 L', \quad (14)$$

$$R = k\frac{F l'}{F' l}\left(\frac{N}{N'}\right)^2 R', \quad (15)$$

$$C = \frac{1}{k^2}\frac{F' l}{F l'}\left(\frac{N'}{N}\right)^2 C', \quad (16)$$

$$B = B', \quad (17)$$

$$H = H'. \quad (18)$$

F', l', N' and k' are here constants which can have arbitrary values. According to equations (9) to (18), the new magnitudes t', E', U', Q', f', L', R', C', B' and H' differ from the original magnitudes only by constant factors.

As a result of the above substitutions, equations (1) to (8) become:

For each branch except that containing the iron core

$$U' = \frac{1}{k}\frac{F'N'}{F N}U\left(\frac{t'}{k}\right) = U'(t'), \quad (1a)$$

$$I' = \frac{dQ'}{dt'}, \quad (2a)$$

$$-E' = L'\frac{dI'}{dt'} + R'I' + \frac{Q'}{C'}, \quad (3a)$$

For the iron cored circuit

$$-E' = N' F'\frac{dB'}{dt'}, \quad (4a)$$

$$4\pi N' I' = H'l' \quad (5a)$$

$$B' = f(H'), \quad (6a)$$

For each mesh $\Sigma(E' + U') = 0$, (7a)

For each junction point $\Sigma I' = 0$ (8a)

The only difference between this new set of equations and the original set is in the addition of an accent to all letters, except to the functional symbol f in equation (6).

The new equations describe the distribution of current and voltage in another network composed of the same circuit and the same core material, but with different network constants (R', L' and C' in place of R, L and C), with other core constants (l', F' and N' in place of l, F and N) and with other external e.m.f's ($U' = U'(t')$ in place of $U = U(t)$). The only factor which has not been changed by this transformation is the magnetic state of the core material at corresponding times.

Since the new set of equations has been derived with the aid of equations (9) to (18), the proportionality between the original and new variables as determined by equations (9), (10), (12) and (13) is in all circumstances maintained. We can, there-

fore, derive the unknowns of the new set of equations from those in the original set by using equations (9), (10), (12) and (13), provided the unknows are known for these initial equations, e.g. as a result of measurement.

The fact that the magnitudes in the original and new sets of equations are connected by equations (9) to (18) may be briefly described by saying that the new set is "equivalent" to the original set.

Since the variations of current and voltage are completely determined by the differential equations together with the initial conditions, it is sufficient to obtain complete equivalence between the two sets of conditions that:

1. The new network constants are connected with the original constants by equations (14), (15) and (16);
2. The new initial currents and charges are connected to the original ones by equations (12) and (13);
3. The new external e.m.f's are connected with the original values by equations (11) and (1a).

The relationship determined by the transformation equations will then be maintained at equivalent times, which implies that the variables in the one case are equivalent to those of the other case except for the constant reduction factors according to equations (9) and (13).

It follows, furthermore, from (10), (16), and (13), (14) that:

$$\frac{{}^1\!/_2\, C' E'^2}{{}^1\!/_2\, C\ E^2} = \frac{{}^1\!/_2\, L' I'^2}{{}^1\!/_2\, L\ I^2} = \frac{l'\ F'}{l\ \ F},$$

i.e. corresponding energies are in the same ratios as the volumes of the iron core belonging to the network.

As the *BH* curve does not lend itself to analytical treatment, the properties of the circuit must be represented by curves or characteristics. Where the characteristics have to be determined for an iron core not yet made, it is sufficient to insert any other core (with arbitrary l', F' and N') in the equivalent network and to plot the characteristics for this equivalent arrangement. According to equations (9), (11) and (17), the characteristics will then apply also to the design under calculation but will be plotted on a different scale. The oscillograph record obtained will also apply to all cases which are equivalent to the actual case investigated, but again be on a different scale.

If, in particular, the external e.m.f's are given by the expression:

$$U\ (t) = p \sin \omega t$$

then it follows from equation (1a) that the external e.m.f's of equivalent designs will be:

$$U'\ (t') = \frac{\omega'}{\omega}\,\frac{F'N'}{F\ N}\ p \sin \omega' t',$$

where $\omega' = \omega/k$ has been substituted.

No attention need be given to the initial conditions, if only the steady state is under investigation. The conditions arising during switching on have then entirely disappeared.

If $U\,(t) = 0$, i.e. we are dealing with an independent network, no attention need be given, on the other hand, to the external e.m.f's. According to (1a), $U'\ (t') = 0$ also in this case, independent of the value of k. The time scale will here be a different one according to the value of k, which is inserted after choosing R', C', Q'_0 and I'_0 in accordance with equations (15), (16), (12) and (13).

The above analysis can be readily applied to cores with more than one winding. In the transformation equations, the number of turns on that winding belonging to the same part of the network as the brach under consideration is then inserted for N and N'.

The mutual inductances, which can then be obtained between branches of the various sections of the network or between branches of the same section, can also be included in equation (2).

In the first case the reduction equation becomes:

$$M_{12} = \frac{l'\,F\,N_1\,N_2}{l\,F'N_1'N_2'}\,M_{12}', \quad \cdots\cdots \quad (19)$$

where the indices relate to the section under consideration and N denotes the number of turns on the corresponding core windings. The second case is a particular case of the first where $N_1' - N_2'$ and $N_1 - N_2$.

In an analogous manner, the transformation equations may be deduced for the constants R_{12} (here $R_{12} \neq R_{21}$) applying to rotating electrical machinery. If the rotational e.m.f., E_1, which is induced in an armature winding belonging to section *1* as a result of a current I_2 flowing through a field winding belonging to section 2, is given by the expression:

$$E_1 = R_{12} I_2$$

we get for R_{12} a reduction factor which is k times the reduction factor for M_{12} in (19).

Transformation equations can also be deduced in certain circumstances for the constants of amplifying valves.

The characteristics for a series of designs of various sizes and shapes can be reduced to a form permitting a direct comparison, viz., by applying equations (9) to (20) so as to reduce them to the equivalent case with $l' = 1$, $F' = 1$, $N_1' = 1$ and $N_2' = 1$. The arrangement is then converted to an imaginary equivalent one with a cubical iron core of 1 cm length of side, where it may be assumed that the iron circuit is closed by a yoke of infinitely high permeability. Each of the windings of this imaginary iron consists of one turn only. The rating

of each condenser and each choke coil of the reduced network is equal to that of the equivalent member of the original network, divided by the volume of the original iron core.

Advance Testing Equipment

It appears worth while to construct a permanent equipment with which all types of equivalent circuits can be set up and tested to assist in arriving at a suitable design of equipment to meet a specific practical purpose. The results of measurement obtained with this equipment can then be converted to the particular case under consideration using the method discussed above. The reduction formulae are, in fact, further simplified by employing this procedure, since l', F', N_1' and N_2' of the testing equipment can be included once and for all in the constant factors.

Furthermore, the transformer of the testing arrangement can be given the most suitable design to simplify measurements as far as practicable. Since, with equivalent networks and when using the same frequency, which should preferably be made equal to 50 cycles, the rating of all branches is proportional to the volume of the iron core, it is advisable to make the core with not too large a volume. This will avoid the voltage, current or power values exceeding the measuring range of the measuring instruments available as well as the need for making the leads too thick or too stiff. Moreover, in this way the ratings of the rheostats, regulating chokes and condensers required in the equipment can be maintained within reasonable limits. The number of turns on the windings can be given any arbitrary value, and should merely be adapted to the characteristics of the instruments.

The materials used for the iron core of the testing arrangement must naturally be the same as that used for the core of the actual piece of equipment being designed. In practice, the same material is, however, always used, viz., high-alloy transformer iron, since its BH curve is extremely suitable for the duties in question [2]), and this material is not too expensive and is also easily obtainable.

A large variety of designs can thus be investigated with a single core of high-alloy transformer iron incorporated in the testing equipment.

[2]) The BH curve of high-alloy transformer iron has in fact a marked turning point, which is necessary for the reliable operation of equipment of this type. As mentioned in the introduction, the BH curves of different consignments of the same sheets are not always exactly similar and this must be taken into consideration in the practical application of the result obtained with small-scale models. In the example discussed below this point is considered.

By using the cathode-ray oscillograph, which is always available for immediate use and requires as little preparation before taking readings as a voltmeter or ammeter, the testing procedure is much simplified, since there is no restriction on the number of turns on the core windings and these can therefore be adapted to the sensitivity of the oscillograph. In consequence, an amplifier is not required in any measurement.

To permit the measurement of non-periodic phenomena with the cathode-ray oscillograph, these can be converted into periodic phenomena, for instance by periodical repetition using a contact disc revolving in synchronism.

With the testing equipment described, the optimum values for all types of designs can be rapidly found for all unknown magnitudes, by taking various combinations of these values in succession and reading off their effect directly on the instruments.

Stabiliser for Compensating fluctuations in mains voltage

A device designed for compensating fluctuations in mains voltage will now be discussed to serve as a concrete example of the general analysis made above.

The circuit diagram of a device of this type is shown in *fig. 1.* On an alteration in the mains

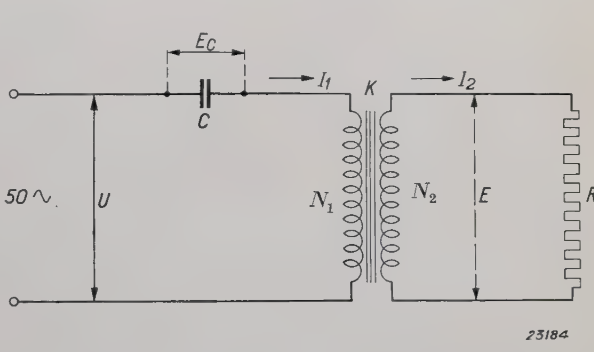

Fig. 1. Circuit diagram of a stabiliser with load resistance. K is the closed iron core; N_1 and N_2 are the number of turns of the coils in the windings. R is the load resistance, and C is a condenser with a potential E_C. U and E are the input and output voltages respectively; I_1 and I_2 are the current intensities.

voltage U, a corresponding change takes place in the primary current, although the magnitude of the iron field remains nearly constant owing to state of saturation of the iron; the same also applies for the output voltage E which is induced by the field in the secondary winding.

The efficiency of the device in relation to its proposed purpose is expressed by the factor of

compensation, i.e. the ratio of the percentage variation in the input voltage to that in the output voltage.

For a device of this type, the output voltage E is plotted in *fig. 2* as a function of the input voltage U with constant R.

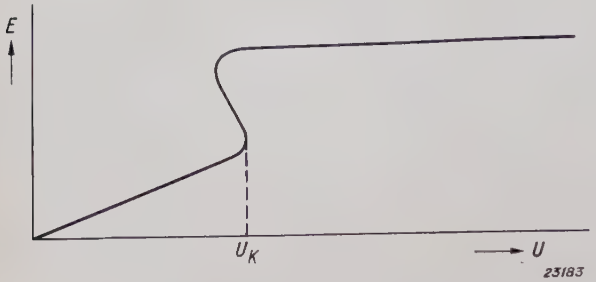

Fig. 2. Characteristic of a voltage stabiliser. U is the effective value of the input voltage; E is the effective value of the output voltage with a constant-resistance load. U_k is the effective value of the output voltage at the lower turning point of the curve. The upper, nearly horizontal, branch of the curve represents the working range.

The device functions as a stabiliser along the nearly horizontal part of the curve. The greater the value of U, the higher must be the ratings of the transformer and the condenser, and hence the higher will be the cost of the equipment. The operating range should, therefore, be located as far to the left as possible, although there is a limit at the point where $U = U_k$, i.e. where the ordinate touches the lower turning point, otherwise the working point could remain fixed in the lower branch of the curve when the mains voltage is applied.

If compensation is to be provided for possible deviations of the BH curve and for fluctuations in mains voltage of 10 per cent in either direction, the working range should be located between about 1.15 U_k and 1.40 U_k, with a nominal mains voltage U of 1.27 U_k.

It is required to arrive at the optimum shape of the E-U curve by selecting a suitable iron core, the optimum number of turns and the best constants of the network, so that the compensation factor will be sufficiently high and the ratings of the condenser and the transformer as low as possible, since these ratings determine the size and cost of the equipment.

The problem appears a very complex one owing to the large number of choices available, and hence the large number of combinations which have to be tested. It appears that tests are required with a series of iron cores of different shapes and sizes, as well as with different numbers of turns in conjunction with a wide range of different capacities.

But with the aid of the general analysis given above it is possible to simplify the problem considerably, because all designs can be referred to the same standard of comparison, viz., by reducing them all to the transformer in the testing equipment. Since as a rule networks of 50 cycles have alone to be considered, the question of a mathematical transformation of frequency can be neglected for the moment and we can hence put $k = 1$. While the original curve is determined by C, R, N_1, N_2, l and F, the number of parameters in the reduced curve has been diminished to two. The circuit shown in fig. 1 shows this to be the case, for if the transformer shown in fig. 1 is always the same with the same values of l', F', N', and N_2', only R' and C' remain variables.

By applying this reduction the problem is thus reduced to the following:

It is required to determine the values of R' and C' such that:

1) With the value of U' lying between 1.15 U'_k and 1.40 U'_k, the factor of compensation shall be sufficiently high, and

2) P_C'/P_R' and P_T'/P_R' shall be as small as possible for $U' = 1.27\ U_k'$. P_C' and P_T' are here the apparent powers of the condenser and the transformer, while P_R' is the watt consumption of the load resistance.

A solution of this problem can be arrived at without calculation, viz., by direct experiments with the testing equipment. For different values of R' and C' the E'-U' curve is plotted and therefrom the values of the three magnitudes in 1) and 2) above are determined. As to be expected, condition 1) is in opposition to that under 2). Hence according to the proposed use of the equipment in question, a compromise must be made between a satisfactory factor of compensation and a reasonably low cost of construction.

When suitable values have finally been selected for R' and C', the corresponding values of I_1', I_2', U', E' and E_C' are found by measurement. Together with the values of U, E and I_2, which are laid down in the specification, the measured values obtained provide all the data required for the design of the equipment. If the power output is, for instance, $E\,I_2 = P_R$ or $E'\,I_2' = P_R'$ respectively, we get:

From equations (10) and (13):

$$F = k_1 \frac{P_R}{l} \quad \ldots \; (21), \text{ where } k_1 = \frac{l'\,F'}{P_R'} \quad \ldots \; (21\text{a})$$

From equations (10), (11) and (13)

$$N_1 = k_2 \frac{U\,l}{P_R} \cdots (22), \text{ where } k_2 = \frac{P_R' N_1'}{U'\,l'} \quad (22a)$$

From equation (13):

$$w_2 = k_3 \frac{l}{I_2} \cdots (23), \quad ,, \quad k_3 = \frac{I_2' N_2'}{l'} \cdot (23a)$$

From equations (10), (11), (13) and (16):

$$C = k_4 \frac{P_R}{U^2} \cdots (24), \quad ,, \quad k_4 = \frac{U'^2}{P_R'} C' \quad (24a)$$

From equations (13) and (22):

$$I_1 = k_5 \frac{P_R}{U} \cdots (25), \quad ,, \quad k_5 = \frac{U'\,I_1'}{P_R'} \cdot (25a)$$

From equation (11):

$$E_C = k_6\,U \cdots (26), \quad ,, \quad k_6 = \frac{E_C'}{U'} \cdot\cdot (26a)$$

Since the magnitudes on the right hand side of equations (21a) to (26a) are given by the testing equipment as the optimum combination of values for obtaining a specified factor of compensation, the constants k_1 to k_3 are known for all cases. The working out of the design is thus reduced to arriving at the values of U, P_R and I_2 in equations (21) to (26) to meet the specification. The length of the iron path l can be arbitrarily chosen and, for instance, adapted to the length of the iron path in an available stamping.

If a complete design has not to be worked out, but merely a rough estimate of the cost is required, it is sufficient to determine the apparent power of the condenser $P_C = I_1 E_C$ and the weight of the core $G = 7.8\,lF$. From equations (25), (26) and (21), we then get:

For the apparent power of the condenser:

$$P_C = k_7\,P_R \cdot\cdot (27), \text{ where } k_7 = \frac{E_C'\,I_1'}{P_R'} \quad (27a)$$

For the weight of the core in grammes:

$$G = k_8\,P_R \cdot\cdot (28), \text{ where } k_8 = \frac{7.8\,l'F'}{P_R'} \quad (28a)$$

These two magnitudes are thus expressed in terms of the rated power P_R which the stabiliser must furnish.

We have limited ourselves to an example in which a resistance and a capacity alone appear as network constants. The advantage of the method of calculation described is, in general, the greater, the less a particular case is susceptible to direct calculation. Thus this method has been found exceptionally useful in cases where pre-magnetised choke coils were used in conjunction with valve tubes.

THE RADIATION INTENSITY OF THE PHILIPS FASTNESS-TO-LIGHT METER

By J. F. H. CUSTERS.

Summary. Comparative measurements of the fading of samples on irradiation with sunlight and in the Philips fastness-to-light meter show that the radiation intensity in the fastness-to-light meter is about 50 times greater than the maximum solar radiation obtainable on a horizontal surface at a latitude of 52 deg.

A new apparatus for testing the fastness-to-light of all kinds of materials has already been described in this review [1]). In that article particular attention was called to the very high intensity of the light to which the sample was exposed and which enabled the fastness-to-light of a material to be determined in a very short time. The present article deals in greater detail with the determination of the ratio of the irradiation times required to obtain the same degree of fading on irradiation with sunlight and with the meter in question. The following experiments were necessary for the determination of this ratio, which has a value of approximately 50:

1) Irradiation for specific periods of time of one or more samples with sunlight and with the light given by the meter.
2) Registration of the amount of sunlight and meter light which is required to obtain a specific degree of fading.
3) Measurement of the fading itself, so as to permit direct comparison of the fading produced by sunlight and in the meter.

During exposure to the sun's rays the samples were placed on a horizontal surface covered with black velvet, *T* in *fig. 1*. Half of each sample was covered with a blackened metal strip. At a distance of 5 cm from the samples a sheet of ordinary window glass *G*, 2 mm thick, was placed, so that the air had free access to the samples.

A circular opening, 4 cm in diameter, was cut in the velvet-covered surface through which the sunlight passed into a cylinder, 15 cm wide and 20cm long, whose internal surface was painted a matt-white. Another circular opening, 2 cm in diameter, was cut in the base of the cylinder, through which a considerable part of the sunlight entering the cylinder was transmitted after repeated reflections at the inner white wall. To prevent sunlight falling directly on this aperture a mattwhite circular disc, 4 cm in diameter, was placed horizontally across the middle of the cylinder. A photo-electric cell was located under the base of the cylinder with its window against the lower opening in the cylinder; the cell was carefully screened against all extraneous light other than that reaching it through the opening. The weak electric current flowing through the cell, which is proportional to the intensity of the incident light, was amplified about 500 times and then registered by a recording milliammeter with a revolving drum. As in the Ulbricht sphere, this current intensity is a measure of the light passing through the aperture, i.e. of the intensity of the illumination falling on the sample, irrespective of the direction of the sun's rays.

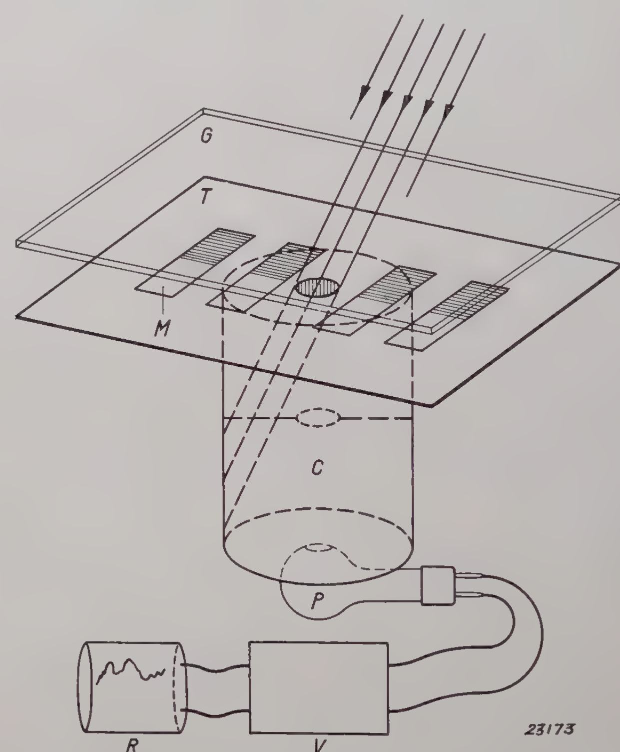

Fig. 1. Arrangement of apparatus for irradiation of different samples with sunlight and for recording the effective amount of solar radiation. *T* - Table, on which the samples were placed. *M* - Sample. *G* - Sheet of window glass. *C* - Cylinder, painted a dull white in the interior. *P* - Photo-electric celle. *V* - Amplifier. *R* - Recording milliammeter.

An arrangement of the type just described had to be used because if the light falls directly on the cell different current intensities are measured according to the angle of incidence. This is due to the fact that the sensitivity of the light-sensitive surface of the cell is not constant over the whole

[1]) J. F. H. Custers, A new apparatus for testing the fastness-to-light of materials. Philips techn. Rev., **1**, 277, 1936. J. F. H. Custers. Ein neuer Lichtechtheitsprüfer. Die Chemische Fabrik **8**, 103 - 105, März 1935.

of its area. By inserting the cylinder between the sample and the cell, a uniform illumination is always obtained over the whole surface of the cell, because the sun's rays are diffusely reflected one or many times at the cylinder wall before reaching the cell. Rotation of the apparatus about the vertical axis of the cylinder thus produces no alteration whatsoever in the current intensity through the cell, so that measurements can be made irrespective of the altitude of the sun and also with a moderately cloudy sky. It is evident that the whole of the light from the sky, i.e. from the sun and the sky generally, falls on the sample. A number of cell-current records are reproduced in *fig. 2* which were registered during two sunny days in June, the majority between 9.a.m. and 4 p.m. Record *A* was obtained on a unusually fine day with a perfectly clear sky and shows that the intensity of illumination increases progressively, apart from very small fluctuations, and diminishes again after midday. (In this article the intensity of illumination is taken as including both the visible and invisible radiation falling in all directions on unit surface of the sample in unit time). Record *B* was also made on a fine, although cloudy, day, the presence of clouds being shown by the marked fluctuations in the curve. The sudden drop in illumination to zero, which occurs at several points of the curve, was due to the top aperture of the cylinder being completely covered for short intervals for the purpose of testing the zero adjustment of the amplifier.

As already stated the deflection on the recorded curves is equal to the intensity of illumination of the samples, multiplied by a constant factor. For the sake of simplicity this factor will be taken as being unity. The area enclosed by the curve and the axis on the one hand and by the ordinates corresponding to two particular times on the other, then gives the amount of radiation which has fallen on unit surface of the samples during the corresponding interval of time; this value can be expressed in ergs per sq cm or in watt-seconds per sq cm.

The samples were irradiated by sunlight on June, 8, 9, 13 and 14, all very sunny days. If the area of each recorded curve is divided by the time of irradiation in hours, the mean intensity of illumination on each of these days is obtained; expressed in arbitrary units this average was 1.43, 1.89, 1.35 and 1.15 on June 8, 9, 13 and 14 respectively and is thus seen to vary considerably [2]). The total radiation falling on the samples on these four days was 27.5 during an aggregate time of irradiation of 19 hrs 35 mins. The maximum intensity of illumination was recorded at 11.45 a.m. on June 9 with an exceptionally clear sky, and was 2.4. With a constant intensity of this maximum value, 27.5/2.4 = 11.5 hrs exposure would have sufficed to produce the same effect as the 19 hrs 35 mins actually taken on the days concerned, i.e. assuming that the effect produced is determined exclusively by the product of the intensity of illumination and the time of irradiation; this is approximately true if the time of irradiation is not too long.

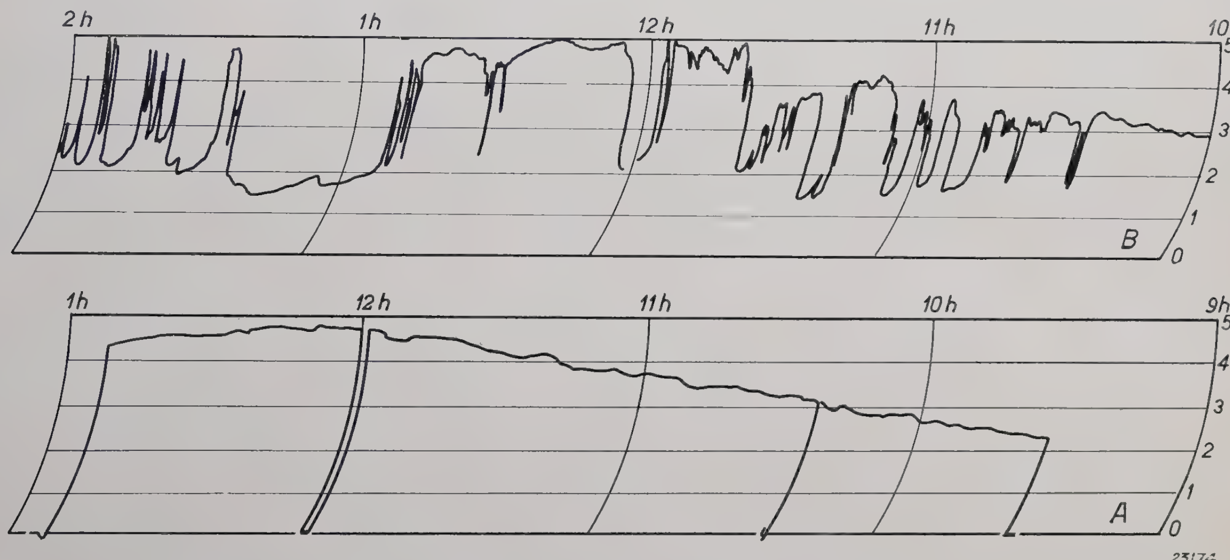

Fig. 2. Records of total radiation falling on unit surface of the sample in unit time. The time was measured in hours. The unit of intensity is arbitrary. *A* was recorded on June 9 and *B* on June 8.

---

[2]) It should be noted that irradiation did not take place during the same hours on each of these days, so that the average values given are not directly comparable. On the other hand, the values 1.89 and 1.15 are comparable, since on June 9 and 14 irradiation took place roughly at the same hours and for the same length of time.

Similar samples were also irradiated in the fastness-to-light meter. As with this instrument the intensity of illumination is constant, it was sufficient to determine the time of irradiation required to produce a change in colour. As will be shown later, an irradiation time of 15.6 mins is required in this instrument to obtain a fading equivalent to that produced by 11.5 hrs exposure to sunlight, provided that the solar radiation is continuously maintained at its maximum value of 2.4, although this optimum condition cannot be realised in practice. The ratio required is therefore $\frac{11.5 \cdot 60}{15.6} = 45$.

To express the fading of the various samples on a numerical basis, reflection measurements were carried out on both the irradiated and original samples at different wave-lengths in the spectrum. A description of the reflection meter used for determining the reflection coefficients cannot be included here, but it should be stated that the direction of the incident light made an angle of about 30 deg. with the normal to the plane of the sample under examination and that the light which was diffusely-reflected along the normal was measured. A piece of white glazed board was taken as a standard of comparison, and its coefficient of reflection assumed to be unity at each wavelength; all samples were referred to this standard.

The reflection curves for the first four samples (*I*: 0.6 per cent Brilliant wool blue FFR extra; *II*: 0.6 per cent Wool blue N extra (825); *III*: 1 per cent Brilliant indocyanine 6 B; and *IV*: 1.5 per cent Fast wool blue GL (974)) chosen from the series of eight types of fast blues issued by the "Deutsche Echtheits Kommission", are given in *fig. 3*. As to be expected the coefficient of reflection R_λ is greater in the blue than in the orange and red. A number of reflection curves of sample *I* after irradiation for various periods in the fastness-to-light meter are given in *fig. 4*. With increase in the time of irradiation, the reflection becomes progressively more uniform throughout the spectrum, i.e. the colour of the sample changes from a saturated blue to a very unsaturated light blue, and the sample bleaches nearly a pure white. Better curves are obtained when, on the basis of the definition of the blackening of a photographic plate, the socalled "reflection-blackness D_λ" is plotted and which is defined by the expression:

$$D_\lambda = \log 1/R_\lambda.$$

If the coefficient of reflection is small (e.g. 0.01), the reflection blackness will be large (e.g. equal to 2) and *vice versa*. D_λ is regarded as a blackening in reflected light. The reflection-blackness curves for sample *I* are plotted in *fig. 5* and can be calculated directly from fig. 4. While the original sample has a low blackness value in the blue and a high blackness value in the red, the blackness value is much smaller in the red and greater in the blue after 8.5 hrs irradiation. These curves are very important because the diminution of D_λ at the maximum of the reflection-blackness curve is to a first approximation proportional to the time of

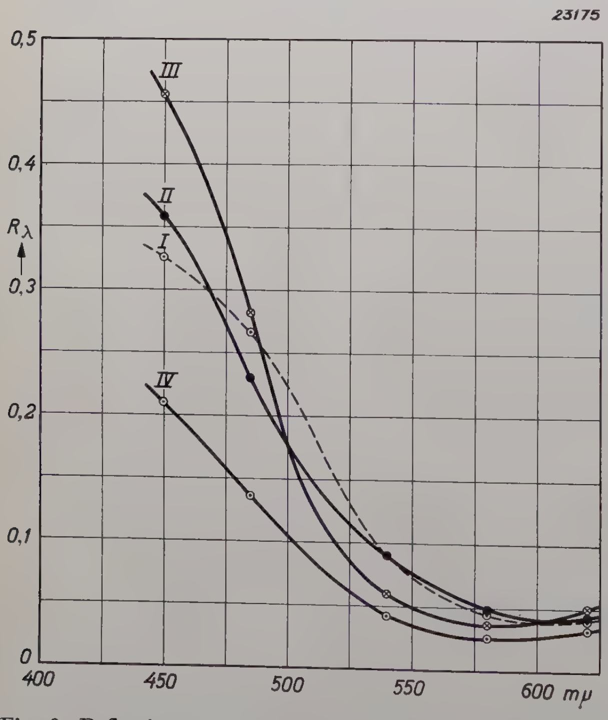

Fig. 3. Reflection curves for four different samples of blue (*I*, *II*, *III* and *IV*).

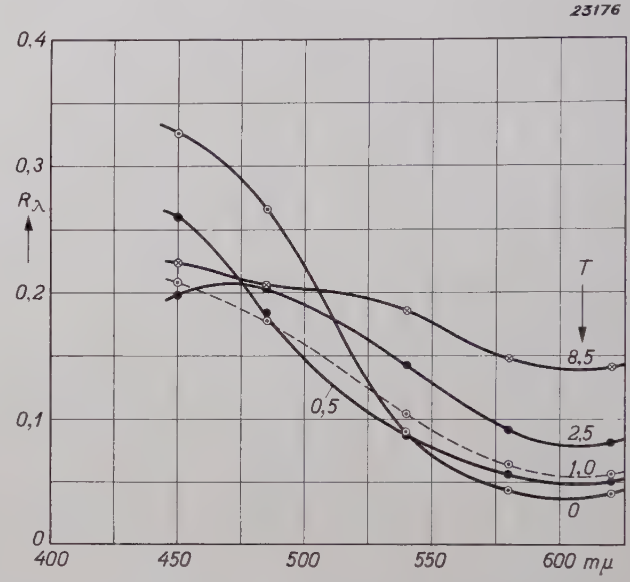

Fig. 4. Reflection curves for sample *I* after irradiation for different times in the fastness-to-light meter. The figures under the letter *T* denote the time of irradiation in hours.

irradiation, provided the latter is not too long. In *fig. 6* ΔD_λ is plotted against the time of irradiation for a wave-length of 620 mμ, and on this curve we made the determination of the irradiation ratio referred to above.

Fig. 7 gives the blackening curves of the original sample *I* and the curve after exposure of the same sample to sunlight. At 620 mμ, D_λ has dropped from 1.382 to 1.334, so that $\Delta D_\lambda = 0.048$. To obtain this alteration in D_λ, irradiation was required for

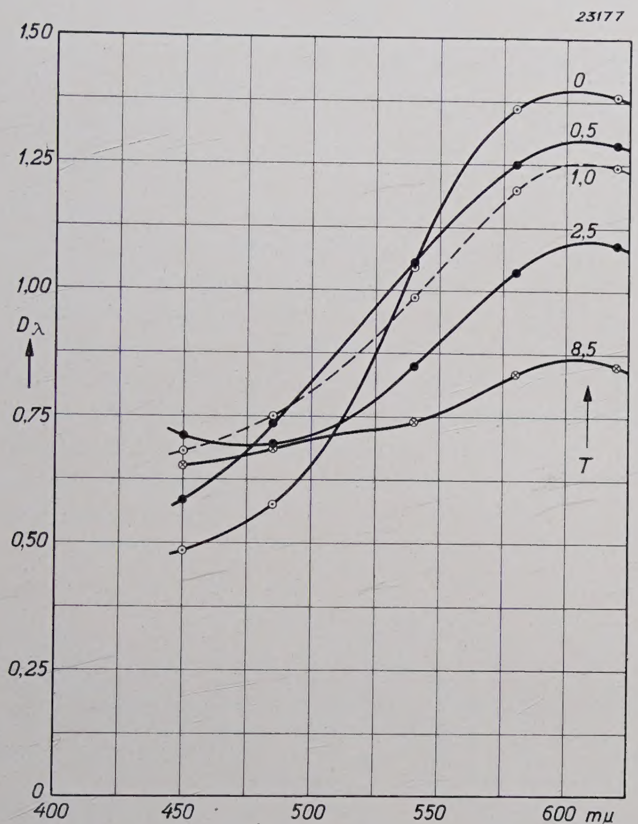

Fig. 5. Reflection-blackening curves for sample *I* for different periods of irradiation in the meter. The figures under the letter *T* denote the time of irradiation in hours.

11.5 hrs at the maximum intensity of 2.4 On irradiation on the fastness-to-light meter D_λ was reduced from 1.382 to 1.290 in 30 minutes, so that $\Delta D_\lambda = 0.092$; thus, in $\frac{0.048}{0.092} \times 30 = 15.6$ mins D_λ has been reduced by 0.048. It follows from this that 15.6 mins irradiation in the meter is equivalent to an irradiation with sunlight at maximum intensity of 11.5 hrs. The irradiation factor for various samples was determined in this way. For some samples it was found to be on the high side and for others on the low side; the average value was 50 with a maximum deviation of $\pm$ 15.

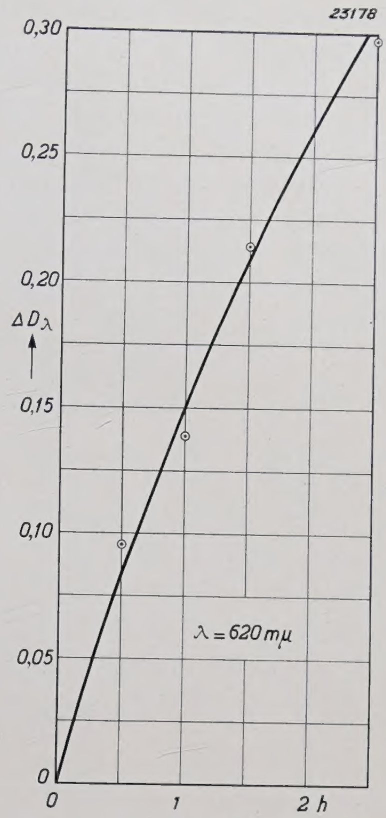

Fig. 6. Reduction in reflection blackening (ΔD_λ) plotted against the time of irradiation in hours at a wave length of 620 mμ.

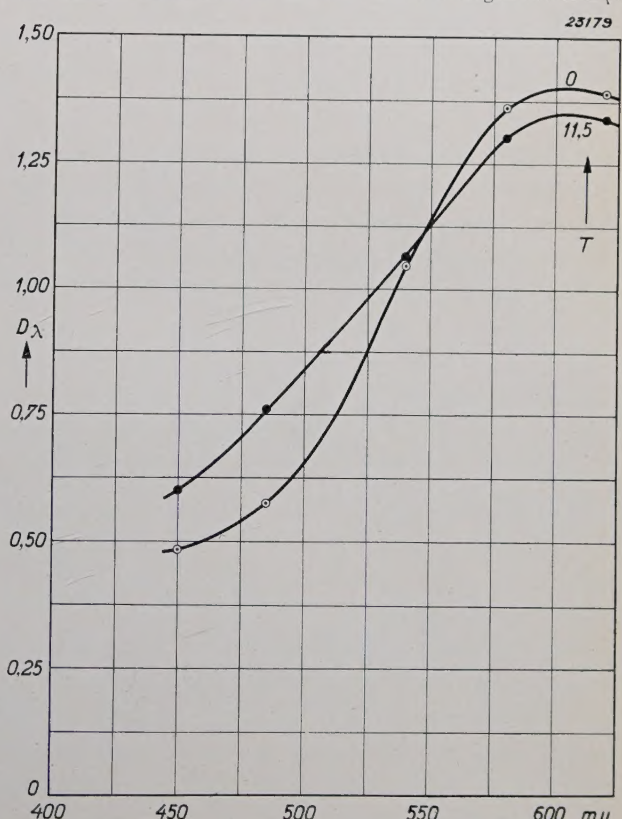

Fig. 7. Reflection blackening curves for sample *I* before irradiation and after 11.5 hours solar irradiation (with maximum solar intensity).

REVIEW OF RECENT SCIENTIFIC PUBLICATIONS OF THE N.V. PHILIPS' GLOEILAMPENFABRIEKEN

No. 1183: A. Bouwers: Convergence of electrons by means of magnetic coils (Physica 4, 200 - 206, March 1937).

The focussing effect of magnetic coils with respect to electron beams is investigated in this paper. The lens effect of a short coil is explained in an elementary manner and the path followed by the electrons is represented. For short and long coils, formulae are derived for the focal distance and for the angle of rotation about the coils. Finally, a number of special cases are considered, such as the borderline case between short and long coils and the effect of a non-homogeneous strong field, by means of which enlarged or reduced images can be obtained.

No. 1184: J. van Niekerk: Einige pharmakologische Untersuchungen mit Salzen von reinem Zirkonium und reinem Hafnium (Naunijn-Schmiedebergs Arch. exp. Pathol. Pharmakol. **184,** 686 - 693, March 1937).

The results of investigations on the pharmacological action of zirconium and hafnium oxychlorides are discussed. Their action in equimolecular quantities appears to be the same with corresponding test objects. The pharmacological effect of zirconium oxychloride is found to be identical with that of the group of zirconium compounds investigated by Marui.

No. 1185: E. M. H. Lips: Over de bewerkbaarheid van perlietisch gietijzer (Metaalbewerking **4,** 21 - 26, March 1937).

The machinability of pearlitic cast iron can be determined without the need for specially-prepared specimens, since the structure already indicates that the machinability is mainly determined by: 1) The hardness of the pearlitic ground mass, which can be determined with a micro-scelerometer, 2) the amount of free graphite, which can be established by chemical analysis, and 3) the distribution of free graphite, which can be studied on an unetched preparation.

No. 1186: P. J. Bouma: Is geel licht minder verblindend dan wit licht? (Wegen, **13,** 132 - 135, March 1937).

In respect of simultaneous glare, yellow and white lights are roughly equivalent, but as regards successive glare and fatigue yellow light is very much better (cf. Philips techn. Rev. **1,** 225, 1936).

No. 1186*: J. W. M. Roodenburg: Der Einfluss der Tageslänge im Zusammenhang mit der künstlichen Pflanzenbeleuchtung im Winter (Ber. deutsch. botan. Ges. **55,** Heft 1, Febr. 1937).

The growth of leaves, which is directly associated with the assimilation of carbon dioxide, is found to be proportional to the quantity of incident light (duration times intensity) for an average irradiation period and intensity. But the growth of blossoms and other similar actino-periodical processes can be promoted by additional illumination with such low intensities that the assimilation of carbon dioxide is barely increased as a result thereof. The length of the day has, of course, a marked effect on the shooting of leaves and peduncles, and thus has an action similar to that of cell-activating hormones. It is probable that the duration of diurnal irradiation affects in some way or other the condition of the growth-promoting substance.

No. 1187: J. L. Snoek and M. W. Louwerse: Magnetic powder experiments on rolled nickel iron (II) (Physica **4,** 257 - 266, Apr. 1937).

The Bitter patterns, which can be obtained from magnetic powders on thin-rolled sheets of nickel iron in the magnetic maximum-anisotropic state when the lines of force issue perpendicularly, are submitted to closer examination, especially along the narrow side of the strip material. On the long sides of the strip, remarkable zigzag patterns are observed with comparatively weak fields, which on a reversal of the field are transformed to complementary patterns, i.e. those in which the lines do not intersect those of the initial patterns. On the rolling plane complex patterns are obtained, in addition to the known parallel strips, but which on reversing the field are not transformed into the

*) There is not a sufficient number of reprints available for distribution of the publications marked *. Reprints of the other publications will on request gladly be supplied by the Administratie van het Natuurkundig Laboratorium, Kastanjelaan, Eindhoven.

corresponding complementary patterns. It is definitely established that the lines on field reversal do intersect. No satisfactory explanation for these phenomena has been advanced.

No. 1188: H. Bruining, J. H. de Boer and W. G. Burgers: Secondary electron emission of soot in valves with oxide cathode (Physica **4**, 267 - 275, Apr. 1937).

When a carbon surface is covered with barium atoms, the capability for secondary emission is increased. However, soot precipitated from a flame, which is composed of very small particles, was found to exhibit a different behaviour. It may be deduced from the change of the secondary emission with time that the barium atoms precipitated on this carbon modification disappear from the surface, with even a moderate electron bombardment. Owing to local heating the barium migrates to soot particles at a greater depth. This migration of the barium is less marked with soot which has been sprayed from a suspension, since in this case the small particles are agglomerated to form large ones, as is confirmed by electron diffraction experiments.

No. 1189: W. Elenbaas: Der Gradient der Überhochdruck-Quecksilberentladung (Physica **4**, 279 - 284, Apr. 1937).

In extra-high pressure mercury discharges, the potential drop per unit of length, i.e. the gradient, is greater than that which would be expected from measurements at one atmosphere pressure on the basis of previously-derived reduction formulae. Some possible causes for this are discussed.

No. 1190: J. H. de Boer: Über die Natur der Farbzentren in Alkalihalogenid-Kristallen (Rec. Trav. chim. Pays-Bas, **56**, 301 - 309, March, 1937).

The equilibrium concentrations of the colour centres found by Mollwö cannot be explained on the basis of the early theory of colour centres which assumed these to be neutral alkali atoms absorbed at the inner surfaces of lattices. According to Schottky, ionic spaces in the lattice and their associated clusters, such as play a part in ionic conduction and diffusion in alkali halides, may also have a bearing on the formation of colour centres. The energy levels of the occupied and unoccupied electron levels in the lattice and of the alkali and chlorine ions which are situated next to the spaces, are such that the colour centres produced by the absorption of light and the penetration of electrons may be regarded as neutral alkali atoms situated at a halogen ionic space. This provides an explanations for the fact that the absorption bands are reproducible and also accounts for the existence of an equilibrium concentration of the colour centres. Defects in the lattice can likewise be places where colour centres are formed, when the absorption bands are broadened or displaced and the equilibrium concentration is exceeded.

No. 1191: J. A. M. van Liempt and W. van Wijk: Die Mikrogasanalyse von Argon-Stickstoff-Mischungen (Rec. Trav. chim. Pays-Bas, **56**, 310 - 314, March 1937).

In this paper a arrangement is described for the quantitative analysis of small quantities of an argon-nitrogen mixture.

No. 1192: M. J. O. Strutt and A. van der Ziel: Erweiterung der bisherigen Messungen der Admittanzen von Hochfrequenz-Verstarkerröhren bis 300 Megahertz (El. Nachr. Techn., **14**, 75 - 80, March, 1937).

Methods are given whereby an "acorn" diode voltmeter can be calibrated with sufficient accuracy for measuring impedances. The various precautions are also discussed which must be taken into consideration in the design of transmitters required to operate efficiently up to 300 megacycles, as well as the adequate screening of the various components of the measuring apparatus. Impedance measurements carried out on shortwave valves, particularly "acorn" pentodes, up to 300 megacycles are also described. It was found that voltage amplification is possible up to 300 megacycles with these valves.

No. 1193: M. J. O. Strutt: Frequency changers in all-wave receivers. The performance of some types (Wireless Eng., **14**, 184 - 192, April, 1937).

This article is an English translation of the paper summarised in Abstract **No. 1177**.

No. 1194: W. G. Burgers: Optische demonstratie van eenige verschijnselen, welke optreden bij de verstrooiing van Röntgen- en electronenstralen door kri-

stallen (Ned. T. Natuurk., **4**, 1 - 14, 33 - 38, 1937).

This article is a report of papers dealing with the demonstration apparatus described in Abstract **No. 1149**. It was shown, *inter alia*, how this apparatus could be used for demonstrating complex electron-diffraction patterns.

No. 1195: J. Alfter and B. Visman: Grundsätzliches zur Automatisierung der Röntgenapparate (Röntgenpraxis, **9**, 244 - 247, April, 1937).

The main purpose of automatic control is to obtain radiographs of optimum quality by ensuring that the X-ray tube is always run at the limiting load when using the best tube for the particular purpose in view. The following advantages accrue:

a) Reproducibility of the quality of the radiation and the time of exposure;
b) Protection of the focal spot against overloads, and safeguards against switching on the apparatus when wrongly adjusted;
c) Manipulation of the apparatus is facilitated.

No. 1196: W. Elenbaas: Ontladungen in Kwikdamp van hooge druk (Ned. T. Natuurk. **4**, 65 - 87, April, 1937).

This paper, which was written for the 1936 Vacation Course in Illumination Technology, presents a survey of discharges through high-pressure mercury vapour.

No. 1197: J. A. M. van Liempt and J. A. de Vriend: The flash time characteristics of indirectly-ignited photographic flash lamps (Physica, **4**, 353 - 360, May, 1937).

Flux-time curves for indirectly-ignited photographic flash lamps with aluminium foil are given. From the standpoint of the practical applications of these lamps those factors are discussed which bear on the use of socalled synchronisers for igniting the lamp and opening the camera shutter after a specific interval.

No. 1198: F. A. Heyn: Radioactivity induced by fast neutrons according to the (n, 2n) reaction (Nature, **139**, 842, May, 1937).

Continuing the investigations referred to in Abstract **No. 1141** in which copper and zinc were bombarded with fast neutrons which caused the expulsion of two neutrons from the nucleus owing to the absorption of one fast neutron, the author has extended these experiments to various other elements. Half-life periods were found for the induced radio-active products obtained in this way, which are in close agreement with those found by Bothe and Gentner when bombarding the same elements with gamma rays, a neutron being expelled in each case. In addition, a number of new radioactive isotopes was found.